Economic Geology, v. 109, pp. 661–687

Lithostratigraphic, Hydrothermal, and Tectonic Setting of the Boundary Volcanogenic Massive Sulfide Deposit, Newfoundland Appalachians, Canada: Formation by Subseafloor Replacement in a Cambrian Rifted Arc

Stephen J. Piercey,[1,†] Gerald C. Squires,[2] and Terry D. Brace[2]

[1] *Department of Earth Sciences, Memorial University of Newfoundland, 300 Prince Philip Drive, St. John's, Newfoundland, Canada A1B 3X5*

[2] *Teck Resources Ltd.–Duck Pond Operations, P.O. Box 9, Millertown, Newfoundland, Canada A0H 1V0*

Abstract

The Boundary volcanogenic massive sulfide (VMS) deposit (~ 0.5 Mt @ 3.5% Cu, 4% Zn, 1% Pb, 34.0 g/t Ag) in the Tally Pond Group, central Newfoundland, represents one of the best preserved, subseafloor-replacement style VMS deposits in the northern Appalachian orogen. The deposit is hosted within a Late Cambrian (~510 Ma) volcanic sequence consisting predominantly of rhyolitic flows and associated volcaniclastic rocks. Footwall strata are dominated by rhyolitic lapilli tuff, tuffs, lesser rhyolite flows, and in situ rhyolite breccias. The hanging wall consists of massive, quartz-bearing, flow-banded lobe and breccia facies rhyolite. The deposit occurs at and below the contact between these two units, and comprises pyrite, chalcopyrite, and lesser sphalerite (and other minerals). Massive mineralization contains abundant clasts of the surrounding host rocks, including chlorite-sericite-quartz–altered rhyolite lapilli and ash. Hydrothermally altered rocks consist of variably intense chlorite with lesser sericite and quartz. Chlorite alteration occurs in a discordant geometry, likely representing hydrothermal upflow zones, and chlorite-sericite-quartz occur as blankets that are parallel to the volcanic stratigraphy, likely representing alteration associated with replacement. The hanging-wall rhyolite flows also contain moderate to intense, pervasive quartz and sericite alteration. Both the hanging wall and footwall are characterized by strong Na_2O-Sr depletions, K_2O-MgO-Fe_2O_3-Ba enrichments, high alteration index values (e.g., Ba/Sr, chlorite-carbonate-pyrite index (CCPI), alteration index (AI)), and enrichments in base metals and volatile metals (e.g., Cu, Zn, Pb, Hg).

The presence of abundant remnant wall-rock and host-rock clasts within the ore, intricate sulfide replacement of laminated porous tuff and sand dikes, replacement fronts in host lithofacies, and intense alteration in both the footwall and hanging wall (where the hanging wall is preserved) are all features consistent with formation of the bulk of the Boundary deposit via subseafloor replacement. The deposit likely formed as a result of cooling of metal-bearing hydrothermal fluids, mixing with ambient seawater and pore water-entrained seawater within the volcanic rocks at a permeability interface between young, unlithified, highly permeable footwall volcaniclastic rocks and relatively impermeable hanging-wall rhyolitic flows. In our model, this permeability boundary was an important feature that promoted subseafloor replacement within the deposit.

Immobile element systematics of rhyolitic rocks from the Boundary deposit lack major differences in primary petrochemistry between hanging-wall and footwall strata. All rocks from the deposit area are subalkalic with transitional Zr/Y ratios (2.8–4.5), La/Sm ratios <1 (normalized to upper crust), and primitive mantle normalized signatures with slightly light rare earth element (LREE)-enriched patterns with flat heavy REE (HREE), and negative Nb, Ti, and Eu anomalies. These geochemical features, coupled with existing Nd-Pb isotope data, zircon inheritance patterns, and geologic information, are consistent with rhyolitic rocks at the Boundary deposit having formed by re-melting of arc basement, with continental crust (or recycled continental crust) present in the source region. It is likely that the deposit and its associated rhyolitic host rocks formed within a Cambrian continental(?) or pericontinental rifted arc along the margin of Ganderia, within the Iapetus Ocean.

Introduction

Volcanogenic massive sulfide (VMS) deposits are one of the best understood mineral deposit types, a result of a long history of mining, exploration, and research on land, but also due to our ability to study actively forming systems on the modern sea floor (Large, 1992; Franklin et al., 2005; Hannington et al., 2005). It is widely accepted that VMS deposits form from the exhalation of metalliferous fluids on the sea floor, as observed in modern sea-floor settings and inferred from ancient rocks. However, in some ancient deposits there appears to be evidence for not only exhalative mineralization, but also replacement of rocks in the subseafloor environment (e.g., Doyle and Allen, 2003). Furthermore, in recent years it has been increasingly recognized that subseafloor replacement is particularly significant in forming some giant- to super-giant and/or high-grade deposits (Squires et al., 1991, 2001; Galley et al., 1993, 1995; Doyle and Huston, 1999; Hannington et al., 1999; Doyle and Allen, 2003; Bradshaw et al., 2008).

Despite the recognition of subseafloor replacement as a potentially important process in VMS deposit genesis, recognizing replacement in ancient VMS deposits is not a trivial task, as primary stratigraphic, facies, and alteration relationships in many ancient deposits commonly are significantly modified by postmineralization deformation and metamorphism. In this paper we provide a field-based reconstruction of lithofacies and hydrothermal alteration for the Boundary

† Corresponding author: e-mail, spiercey@mun.ca

*A digital supplement to this paper is available at http://economicgeology.org/ and at http://econgeol.geoscienceworld.org/.

0361-0128/14/4205/661-27

Submitted: June 15, 2012
Accepted: July 6, 2013

VMS deposit (~0.5 Mt @ 3.5% Cu, 4% Zn, 1% Pb, 34.0 g/t Ag), which occurs in the Tally Pond Group, Central Mobile belt, Newfoundland Appalachians, Canada. Although a relatively small deposit, it represents an excellent natural laboratory for understanding subseafloor replacement processes, largely because of its flat-lying nature and exceptional preservations of stratigraphic, alteration, and lithofacies patterns. Furthermore, we present lithogeochemical data that provide key insights into alteration processes and the tectonic environment of formation of the Boundary deposit in the Appalachian orogen.

Regional Geologic and Metallogenic Setting

The Boundary VMS deposit is located within the Newfoundland Appalachians (Fig. 1), which is divided into four tectonostratigraphic zones, from west to east (Williams, 1979; Williams et al., 1988; Hibbard et al., 2004): the Humber, Dunnage, Gander, and Avalon zones. The Dunnage zone, the central portion of the orogen in Newfoundland, also termed the Central Mobile belt, represents vestiges of the Iapetus Ocean and comprises arc, back-arc, and ophiolitic rocks that formed along the margins of Laurentia (Notre Dame subzone) and Gondwana (Exploits subzone) in the Cambrian to Ordovician (Fig. 1; Swinden et al., 1989; Swinden, 1991; Kean et al., 1995; van Staal and Colman-Sadd, 1997; Evans and Kean, 2002; Rogers and van Staal, 2002; Rogers et al., 2006, 2007; van Staal, 2007). The Notre Dame and Exploits subzones subsequently were accreted to the Laurentian and Gondwanan margins during the Taconic and Penobscot orogenies in the Middle Ordovician, and to each other during the terminal stages of the Taconic orogeny in the Late Ordovician (van Staal, 2007; Zagorevski et al., 2007a).

The Dunnage zone (Central Mobile belt) and equivalents in the United States are host to most of the VMS deposits in the Appalachian orogen, including those of the world-class Bathurst mining camp in New Brunswick (Goodfellow et al., 2003), and past-producing deposits of the Buchans mining camp (Thurlow, 2010). The Dunnage zone also contains numerous other currently producing (e.g., Duck Pond) and past-producing (e.g., Little Bay) deposits, as well as those at various stages of exploration, from grassroots to near production (e.g., Boundary; Fig. 1). In central Newfoundland, VMS

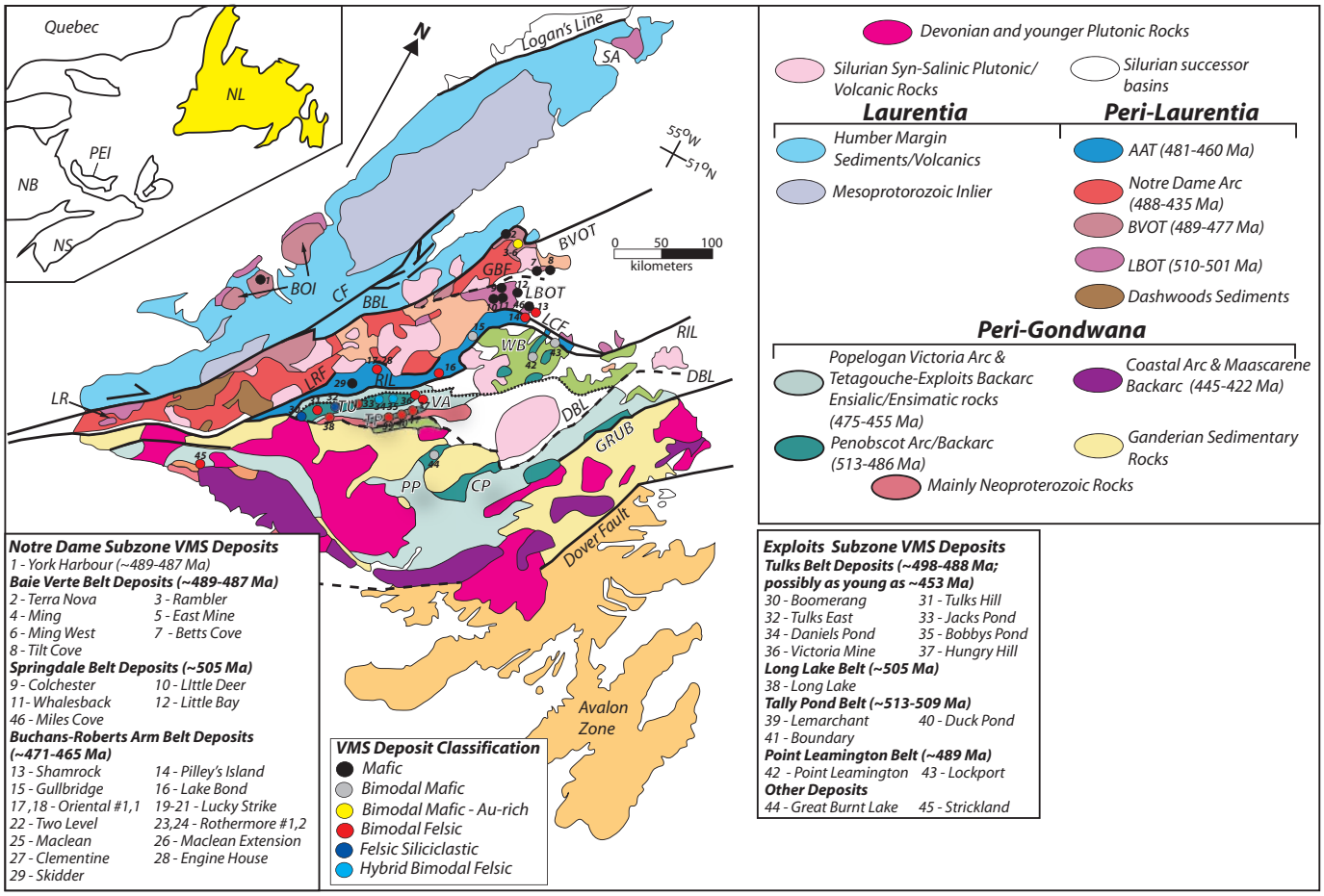

FIG. 1. Geologic map of the Newfoundland Appalachians with tectonostratigraphic zones, accretionary tracts, VMS deposits, their classifications, and associated belts. Map tectonostratigraphy modified from van Stall (2007) and van Staal and Barr (2012). VMS deposit classification from Piercey (2007) and Hinchey (2011). Abbreviations: BBL = Baie Verte Prompton Line; BOI = Bay of Islands; BVOT = Baie Verte Oceanic Tract; CF = Cabot fault; CP = Coy Pond Complex; DBL = Dog Bay Line; GBF = Green Bay fault; GRUB = Gander River ultramafic belt; LBOT = Lushs Bight oceanic tract; LCF = Lobster Cove fault; LR = Long Range; LRF = Lloyds River fault; PP = Pipestone Pond Complex; RIL = Red Indian Line; SA = St. Anthony; TP = Tally Pond belt; TU = Tulks volcanic belt; VA = Victoria arc; WB = Wild Bight Group.

deposits are hosted in both the Notre Dame and Exploits subzones (Fig. 1). Deposits occur north of the Red Indian Line, a major Late Ordovician suture between the Exploits and Notre Dame subzones, and within the Notre Dame subzone, and include deposits hosted in ~510 Ma Lushs Bight Group; ~485 Ma Betts Cove and Bay of Islands complexes, and deposits within the ~485 Ma Rambler-Ming mining camp; and the ~471 to 465 Ma deposits of the Buchans-Roberts Arm belt (Dunning and Krogh, 1985; Dunning et al., 1987; Jenner et al., 1991; Kean et al., 1995; van Staal, 2007; Skulski et al., 2008, 2010). South of the Red Indian Line, within the Exploits subzone, VMS deposits occur in the ~513 to 509 Ma Tally Pond belt; the ~505 Ma Long Lake belt; the ~498 to 491 Ma Tulks volcanic belt; and the ~488 to 485 Ma Wild Bight Group (Figs. 1, 2; Dunning et al., 1991; MacLachlan and Dunning, 1998a, b; Zagorevski et al., 2007b; Hinchey and McNicoll, 2009; McNicoll et al., 2010).

The Boundary deposit is hosted within the Victoria Lake Supergroup (Evans and Kean, 2002). Historically, this supergroup was divided into two main volcanic belts: the Tally Pond and Tulks volcanic belts (Evans and Kean, 2002). More recently, it has been subdivided into six fault-bounded packages, including, from east to west (Fig. 2) the following: the Tally Pond Group (~513–509 Ma; Dunning et al., 1991; McNicoll et al., 2010); the Long Lake Group (~506 Ma; Zagorevski et al., 2007b); the Tulks Group (~498–487 Ma; Evans et al., 1990; Evans and Kean, 2002); the Sutherlands Pond Group (~462 Ma; Dunning et al., 1987); and the Pats Pond and Wigwam Brook groups (~488 and ~453 Ma, respectively; Zagorevski et al., 2007b). VMS deposits occur in the Tulks, Long Lake, and Tally Pond groups (Hinchey, 2007, 2008; Hinchey and McNicoll, 2009).

The Tally Pond Group is host to the Boundary VMS deposit, the producing Duck Pond deposit (resources for Duck Pond + Boundary 4.08 Mt @ 3.29% Cu, 5.68% Zn, 0.9% Pb, 59.3 g/t Ag, 0.9 g/t Au), as well as the Lemarchant deposit (Figs. 2, 3) (Squires et al., 1991, 2001; Wagner, 1993; Evans and Kean, 2002; Squires and Moore, 2004). The Tally Pond Group has been subdivided into two informal formations: the Bindons Pond formation and Lake Ambrose formation (Rogers and van Staal, 2002; Rogers et al., 2006). The Lake Ambrose formation is broadly equivalent to the Lake Ambrose basalts of Dunning et al. (1991), and is basalt-dominated, consisting of pillowed and massive flows, volcaniclastic rocks, and lesser felsic and sedimentary rocks (Kean and Evans, 1986; Evans and Kean, 2002; Rogers and van Staal, 2002; Rogers et al.,

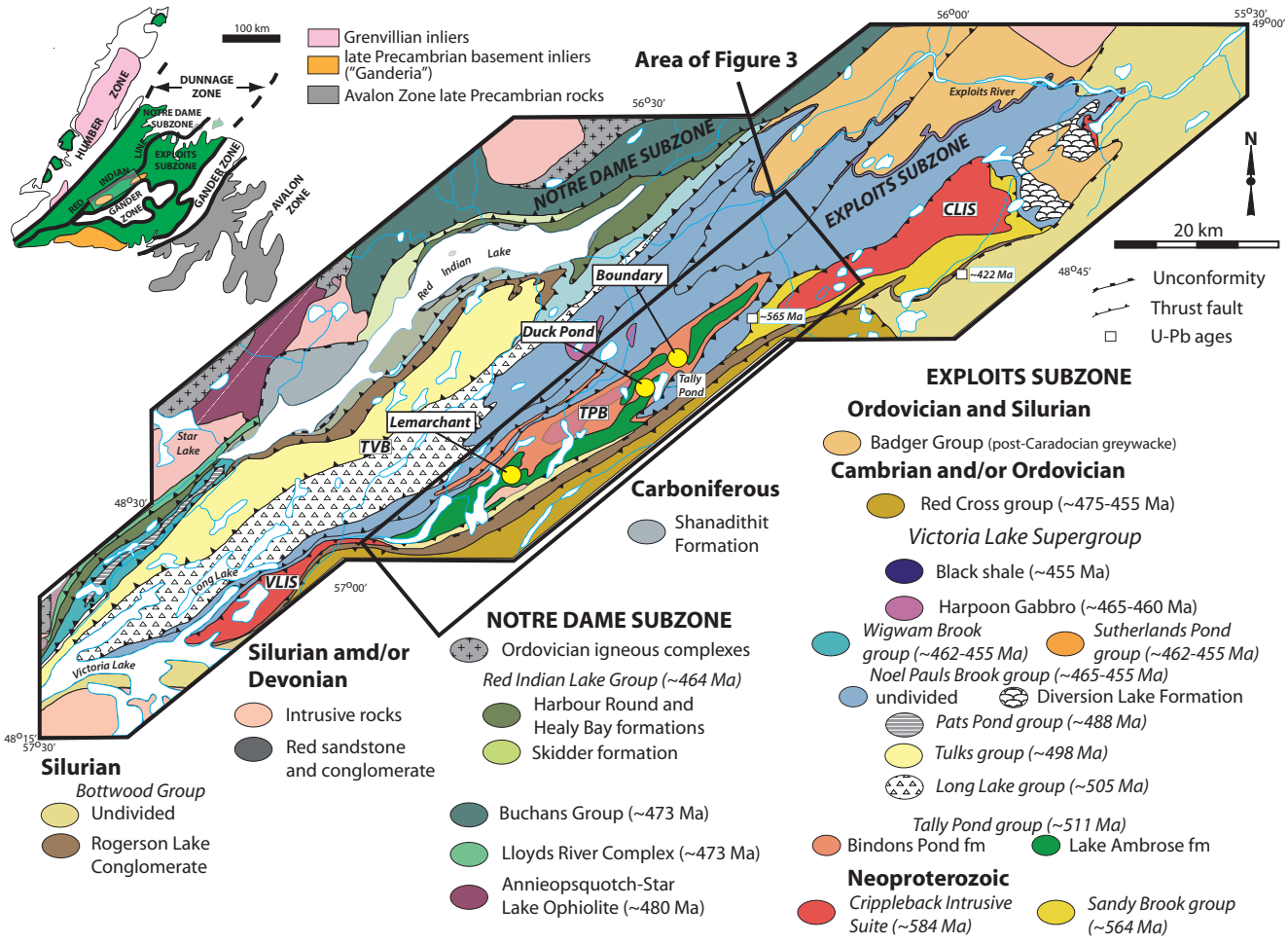

FIG. 2. Geologic setting of the Victoria Lake Supergroup and the Tally Pond group, outlining different VMS deposits in the Tally Pond group. Diagram modified from McNicoll et al. (2010).

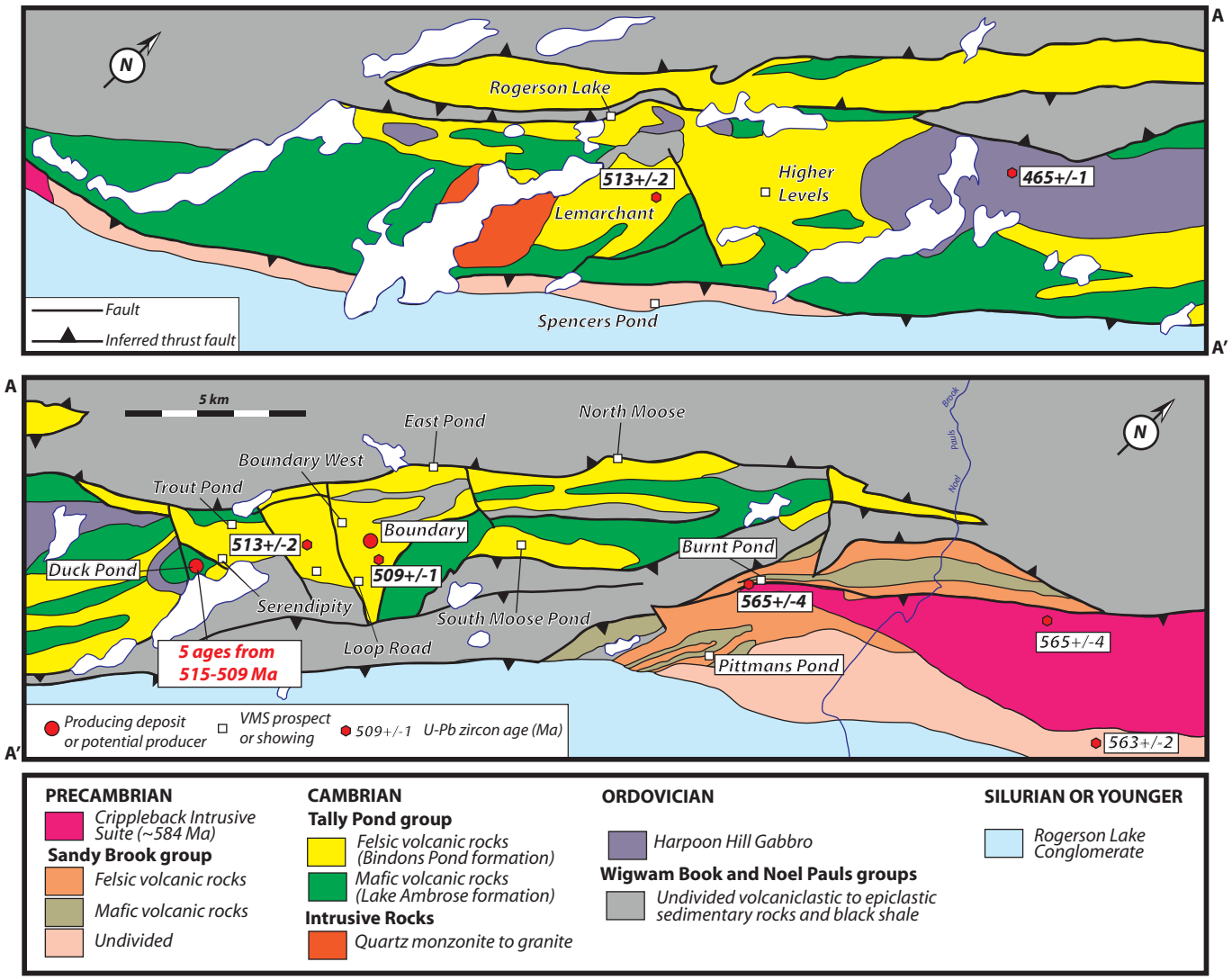

FIG. 3. Geology of the Tally Pond group and associated rocks with the distribution of VMS mines, deposits, and prospects. Diagram modified from McNicoll et al. (2010).

2006). The Bindons Pond formation is felsic-dominated and comprises rhyolitic flows, volcaniclastic rocks, and carbonaceous clastic sedimentary rocks (Kean and Evans, 1986; Evans and Kean, 2002; Rogers and van Staal, 2002; Rogers et al., 2006). Generally, the Lake Ambrose formation is stratigraphically below the Bindons Pond formation (Fig. 3; Kean and Evans, 1986; Evans and Kean, 2002; Rogers and van Staal, 2002; Rogers et al., 2006). Uranium-Pb zircon ages for the Lake Ambrose formation are ~513 Ma, whereas those for the Bindons Pond formation are ~509 Ma; the latter formation hosts mineralization at both the Duck Pond and Boundary deposits (McNicoll et al., 2010).

Stratigraphy and Lithofacies

Stratigraphy, lithofacies, mineralization, and alteration in the Boundary deposit were documented using drill cores, graphic drill logs, and stratigraphic sections. The Boundary deposit is relatively flat lying (Fig. 4); therefore, the sections shown in Figures 5 through 8 represent true thicknesses. Three main zones are recognized: the North zone, South zone, and Southeast zone (Fig. 4). In all zones, mineralization subcrops beneath a veneer of glacial till that is meters thick, particularly in areas where the deposit is not covered by hanging-wall rhyolitic rocks. Locations of the cross sections and long sections are shown Figure 4.

General stratigraphy

The Boundary deposit occurs at and below the contact between a hanging-wall quartz-phyric assemblage of flow-banded rhyolite flows and breccias (lobe and breccia facies rhyolites) with lesser tuff, and a footwall of aphyric rhyolitic lapilli tuff and tuff (Figs. 4–9). Most holes in the deposit are relatively shallow and do not penetrate significantly below the lapilli tuff unit; however, in stratigraphically deeper holes the lapilli tuff are interlayered with aphyric rhyolite flows, rhyolite breccias, and distinctive, jigsaw-fit, aphyric rhyolite breccias (App. Fig. A1, in the digital supplement) that are similar to those in the footwall of the Duck Pond and Lemarchant

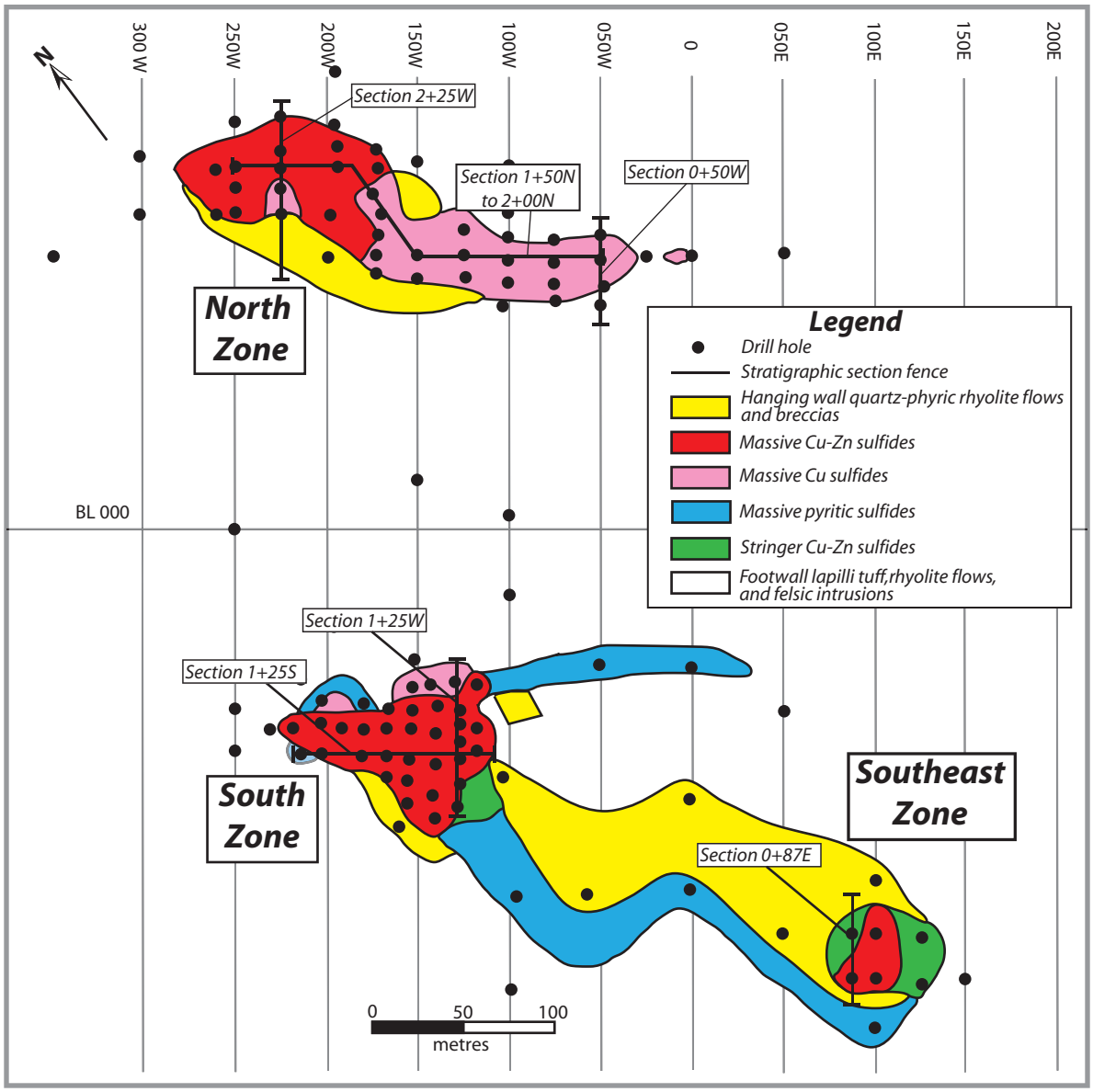

FIG. 4. Boundary deposit surface geology plan map with distribution of sulfide mineralization types, and locations of sections in Figures 5 to 8. Diagram modified from Squires et al. (2001).

deposits (Squires et al., 2001; Moore, 2003; Squires and Moore, 2004; Copeland et al., 2009). The aphyric rhyolites and breccias are interlayered with pillow basalt in even deeper drill holes (e.g., TP88-02 and -52). All units are cut by intrusions of altered quartz-feldspar porphyry. The stratigraphy, facies, relationships, alteration, and mineralization are consistent in all the zones of the deposits (Figs. 5–9).

Lithofacies

Lithofacies are shown on the stratigraphic sections and drill core sections outlined in Figures 5 to 8, with photographs and photomicrographs of the various lithofacies in Figures 9 and 10. The volcaniclastic lithofacies are classified using the classification of Fisher (1966), which has recently been updated by White and Houghton (2006). These classifications are nongenetic and based entirely on clast size and abundance with no implication for the nature or mechanism of emplacement.

Lobe and breccia-facies rhyolite: Lobe and breccia-facies rhyolite is brown (weathered?) to gray and dominated by quartz-phyric, flow-banded rhyolite lobes with marginal breccias (Fig. 9A, B). Most lobes are massive and grade upward (uphole and stratigraphically) into more brecciated to tuffaceous units with flow-banded clasts containing quartz and spherulites (Fig. 10). Most of the brecciated units are strongly altered so that intraclast domains are completely replaced by chlorite and/or quartz (Fig. 9B). This unit is locally cut by pyrite and chalcopyrite stockwork, and regionally (i.e., Boundary West prospect) overlain by Zn-rich pyritic mudstone and mineralized mafic flows.

Lapilli tuff to tuff: Aphyric rhyolitic lapilli tuff is the dominant footwall host to the Boundary deposit (Figs. 5–8). One variant of lapilli tuff consists of clast-supported lapilli tuff with

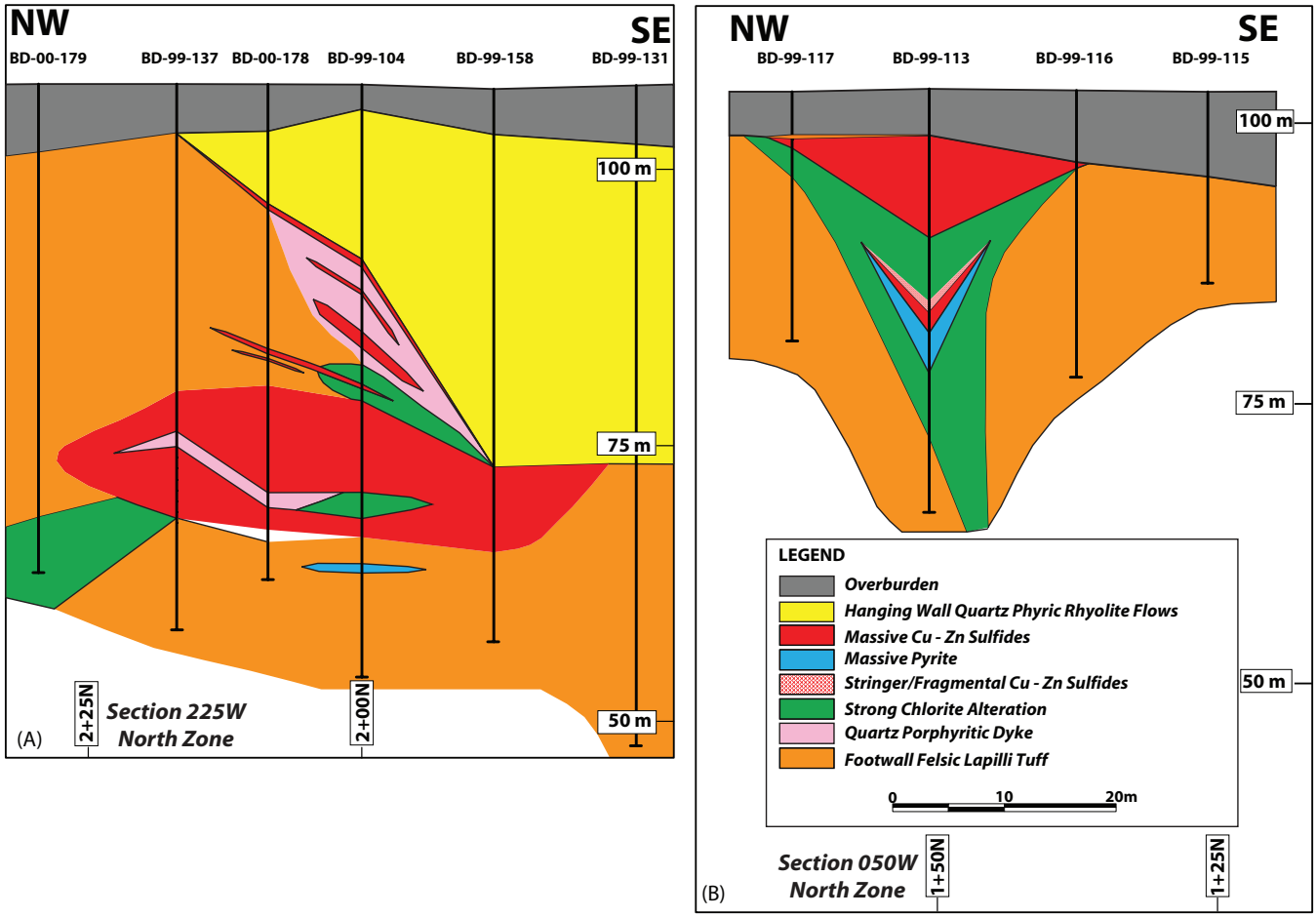

FIG. 5. Cross sections through the North zone of the Boundary deposit. Locations of sections shown on Figure 4. Modified from Squires et al. (2001) and Aur Resources (unpub. sections).

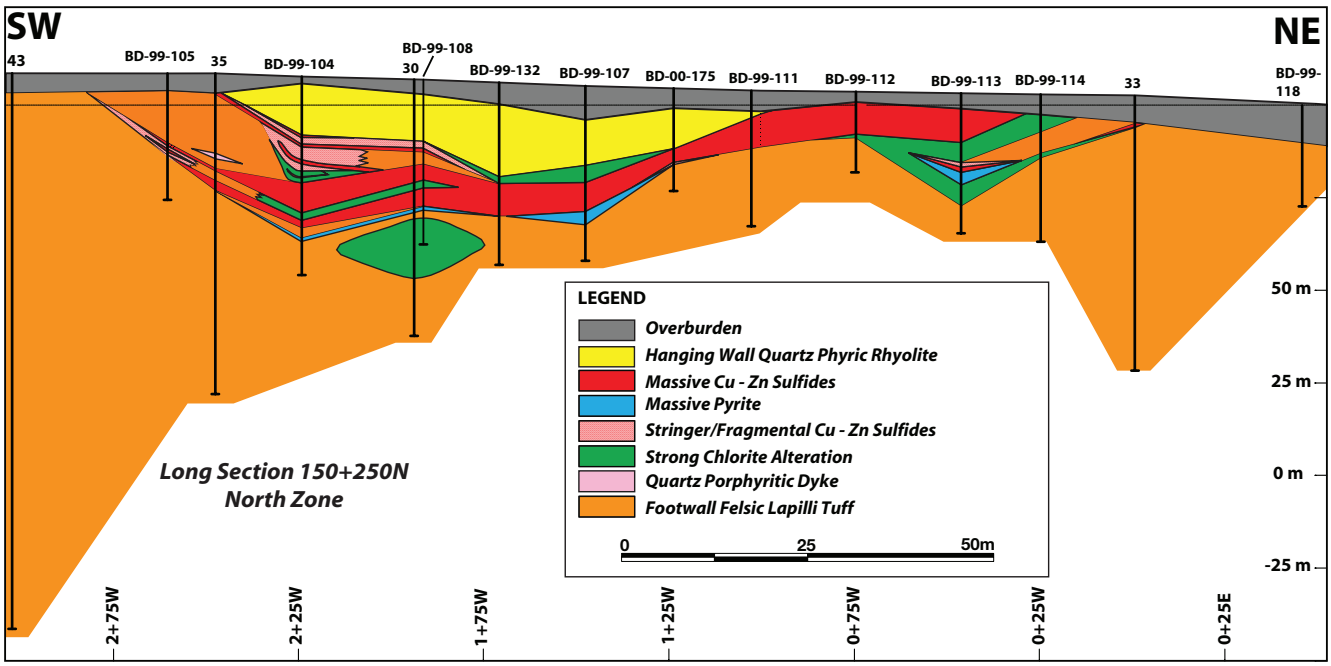

FIG. 6. Long section through the North zone of the Boundary deposit. Locations of section shown on Figure 4. Modified from Squires et al. (2001) and Aur Resources (unpub. sections).

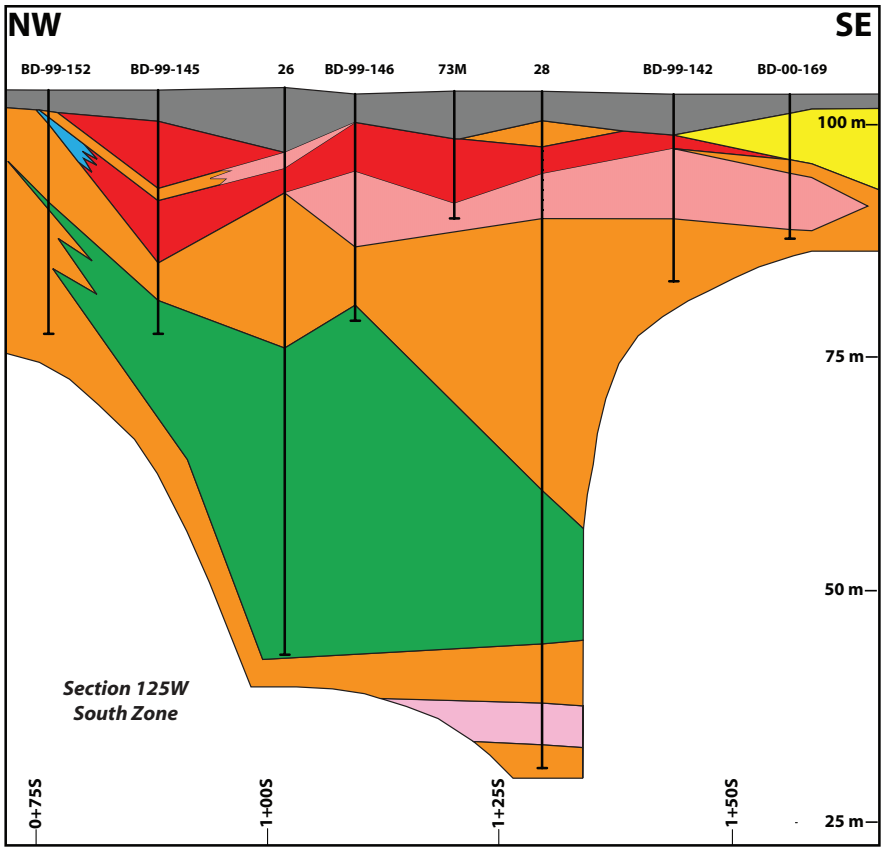

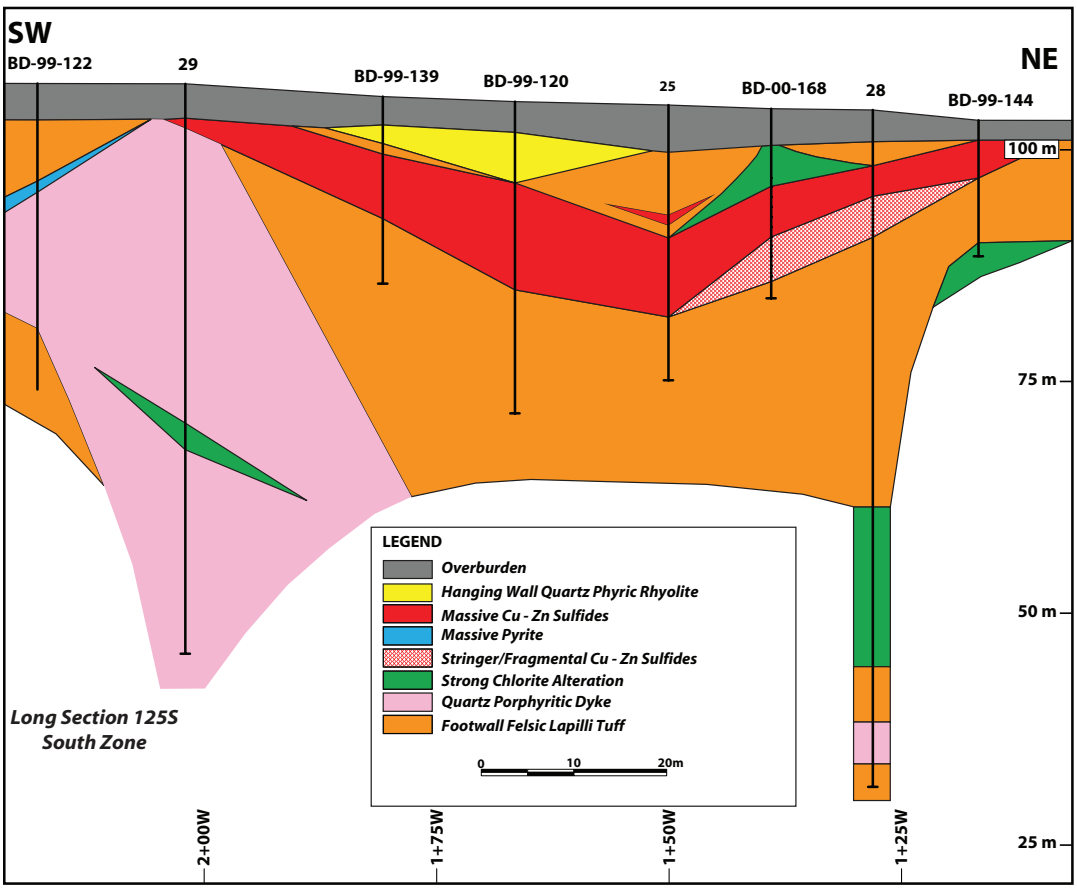

FIG. 7. Cross sections through the South zone of the Boundary deposit. Locations of sections shown on Figure 4. Modified from Squires et al. (2001) and Aur Resources (unpub. sections).

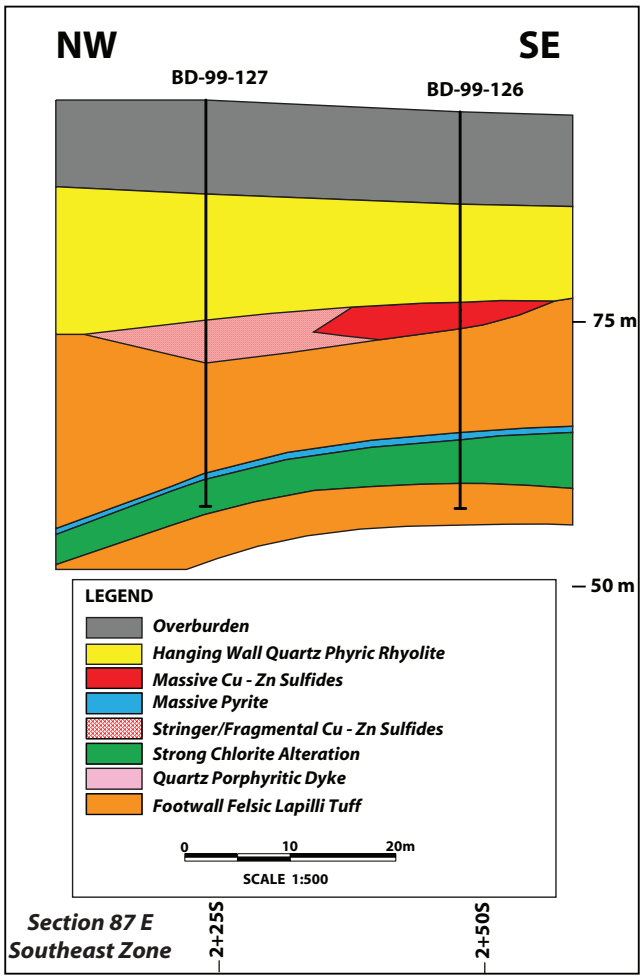

FIG. 8. Cross sections through the Southeast zone of the Boundary deposit. Locations of sections shown on Figure 4. Modified from Squires et al. (2001) and Aur Resources (unpub. sections).

rounded to subrounded clasts of aphyric rhyolite, intraclast ash, some dark black to gray rhyolitic fragments, flow-banded rhyolite clasts, and minor argillite (Figs. 9C–E, 10). Clasts within these units often exhibit relict spherulitic textures, and are often associated with relict glass shards and perlitic textures, suggesting that they were partly glassy when they were emplaced (Fig. 10). The lapilli tuff grade into matrix-supported lapilli tuff with rounded rhyolitic clasts supported within a gray ash matrix, and in places grade further into tuff (Fig. 9F). Matrix-supported lapilli tuff to tuff are significantly less abundant than the clast-supported lapilli tuff in the immediate footwall, but increase in abundance in deeper holes (e.g., TP88-052; App Fig. A1). Deeper holes in the deposit contain both clast- and matrix-supported lapilli tuff, many of which are well sorted and show graded bedding (App Fig. A1).

Jigsaw-fit tuff breccia: Jigsaw-fit tuff breccia is virtually identical to those in the footwall and that host mineralization in the Duck Pond deposit (Squires et al., 1991; Squires et al., 2001). The breccias consist of white to gray, aphyric rhyolite clasts with minor interfragment felsic ash (Fig. 9G, H). Fragments are polygonally jointed to subangular; the breccias are, for the most part, clast supported (Fig. 9G). The jigsaw-fit breccias are more abundant in deeper parts of the deposit and are associated with massive rhyolite flows and flow-top angular rhyolite fragment breccias (e.g., hole TP88-052; App. Fig. A1).

Rhyolite flows and flow breccias: Aphyric rhyolite flows occur as a series of relatively densely packed, gray to white, massive to flow-banded, aphyric rhyolite flows that grade upward into breccias containing flow-banded rhyolite clasts, black relict glass to pumiceous clasts, and ash (App. Figs. A1, A2A, B).

Quartz-feldspar porphyry dikes: Quartz-feldspar porphyry dikes and intrusions of all types are relatively rare in the Boundary deposit, but locally intrude both the lapilli tuff and lower footwall felsic volcanic and volcaniclastic units (Figs. 5, 7; App. Fig. A1). Quartz-feldspar porphyries are gray to white with sharp margins, exhibit minor sericite-quartz alteration, and are similar to those at the Duck Pond deposit; locally they display peperite textures (App. Fig. A2).

Pillow lavas: Mafic lavas are relatively uncommon in the Boundary deposit stratigraphy, except for the lowermost parts of holes TP88-02 and TP88-52 (App. Fig. A1). Here, pillow lavas are intercalated with predominant felsic volcanic rocks (App. Fig. A1). The pillow lavas are gray-green to brown, amygdaloidal, and exhibit variable bleaching (silicification) and Fe-carbonate alteration; some of the pillows have quartz patches and chlorite- and quartz-filled amygdules (App. Fig. A2).

Lithofacies variations: Given the short depth of most of the drill holes at the Boundary deposit, there are very few lithofacies variations that can be discerned. Nevertheless, some general relationships are evident. In the North zone, thicknesses of the hanging-wall lobe and breccia facies rhyolites increase toward the southeast, broadly coinciding with the thickest accumulations of massive sulfide, thus potentially reflecting eruption into a depression, possibly bounded by a synvolcanic fault (Fig. 5). Notably, in regional holes and deeper in the stratigraphy, footwall strata change from volcaniclastic to more coherent flows and intrusions, and to associated coarse, jigsaw-fit breccias and volcaniclastic rocks (App Figs. A1, A2). A similar case appears to exist for the South and Southeast zones, where the footwall to mineralization contains more flows and intrusive rocks (Figs. 7, 8).

Mineralization and alteration

Mineralization: In the Boundary deposit, mineralization occurs in the North, South, and Southeast zones and is dominated by Cu-Zn-rich massive sulfide with variable amounts of base-metal–poor pyritic sulfide (Figs. 5–8). Pyrite-rich massive sulfide is less abundant compared to the Duck Pond deposit, and occurs primarily in the basal portions of the various zones (Figs. 5, 6); however, in rare cases, it also is distal to the Cu-Zn mineralization (Fig. 7). Most sulfide occurs at the contact between the hanging-wall, quartz-phyric lobe and breccia facies rhyolite and footwall lapilli tuff (Figs. 5–8). Mineralization is not one continuous lens at this contact, but instead forms a series of sheets and lenses that are conformable to semiconformable to stratigraphy, at the hanging-wall–footwall contact and within 10 m vertically below this contact, typically within porous footwall lapilli tuff and coarser fragmental units (Fig. 5–8). The multiple horizons typically

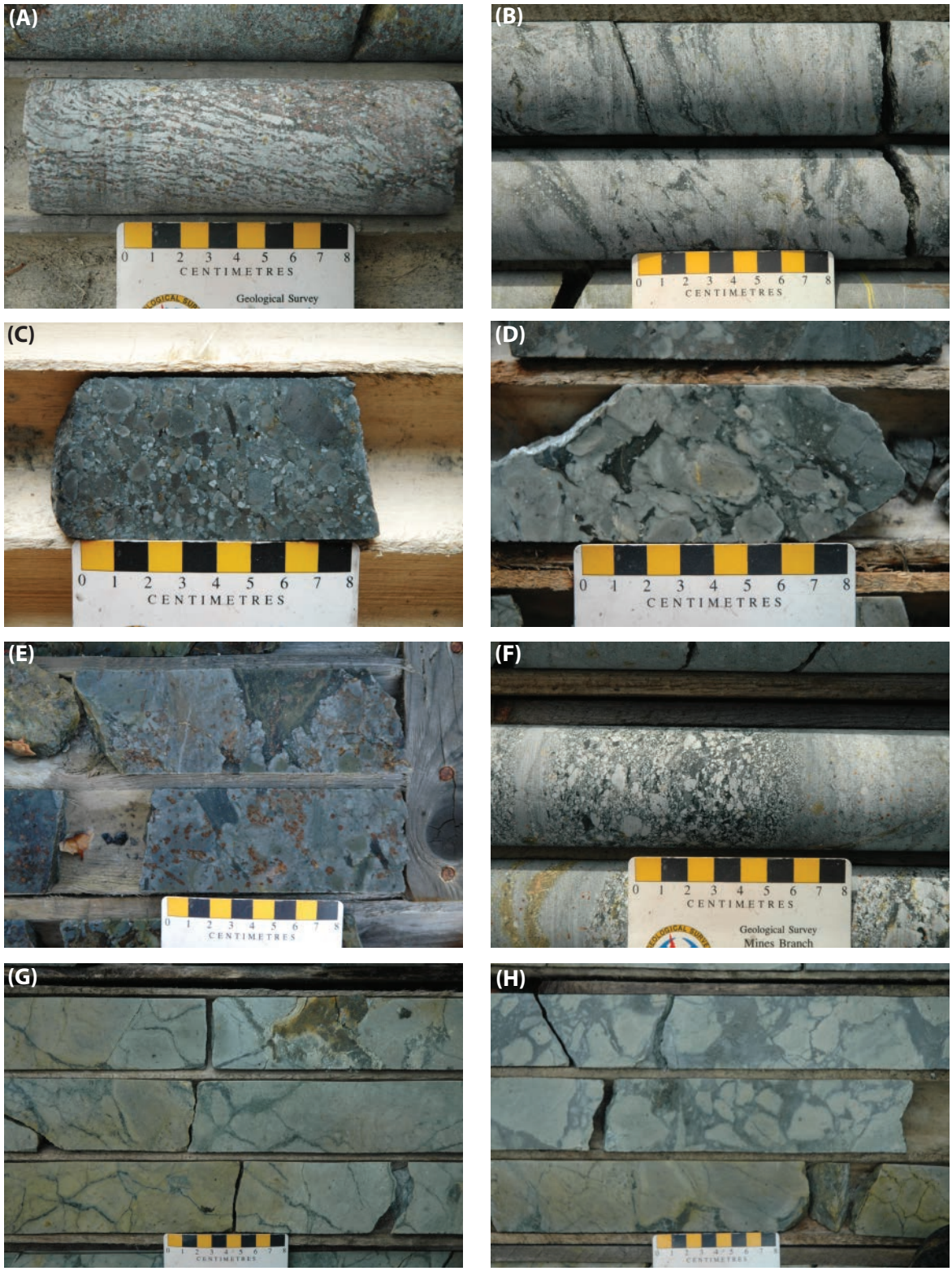

FIG. 9. Host rocks to the Boundary VMS deposit. (A) Hanging-wall flow-banded margin to a lobe and breccia facies rhyolite. (B) Hanging-wall rhyolite flow margin with black zones (false fiamme in a pseudoclastic texture; McPhie et al., 1993) that contain spherulites (white spots). (C) Footwall granular tuff to lapilli tuff with interclast ash that has been partially replaced by chlorite (black). (D) Footwall, clast-supported coarse lapilli tuff with concentrically altered grains and interclast ash and glass shards altered to chlorite (see also Fig. 10D). (E) Deeper footwall flow-banded rhyolite with hyaloclastite that is altered to chlorite (black; see also App. Fig. A1). (F) Bedded footwall fine-grained tuff to lapilli tuff. (G) Deep footwall, aphyric rhyolite with polygonal jointing. (H) Hyaloclast-rich aphyric rhyolite from the deeper footwall with abundant chlorite alteration of interclast ash.

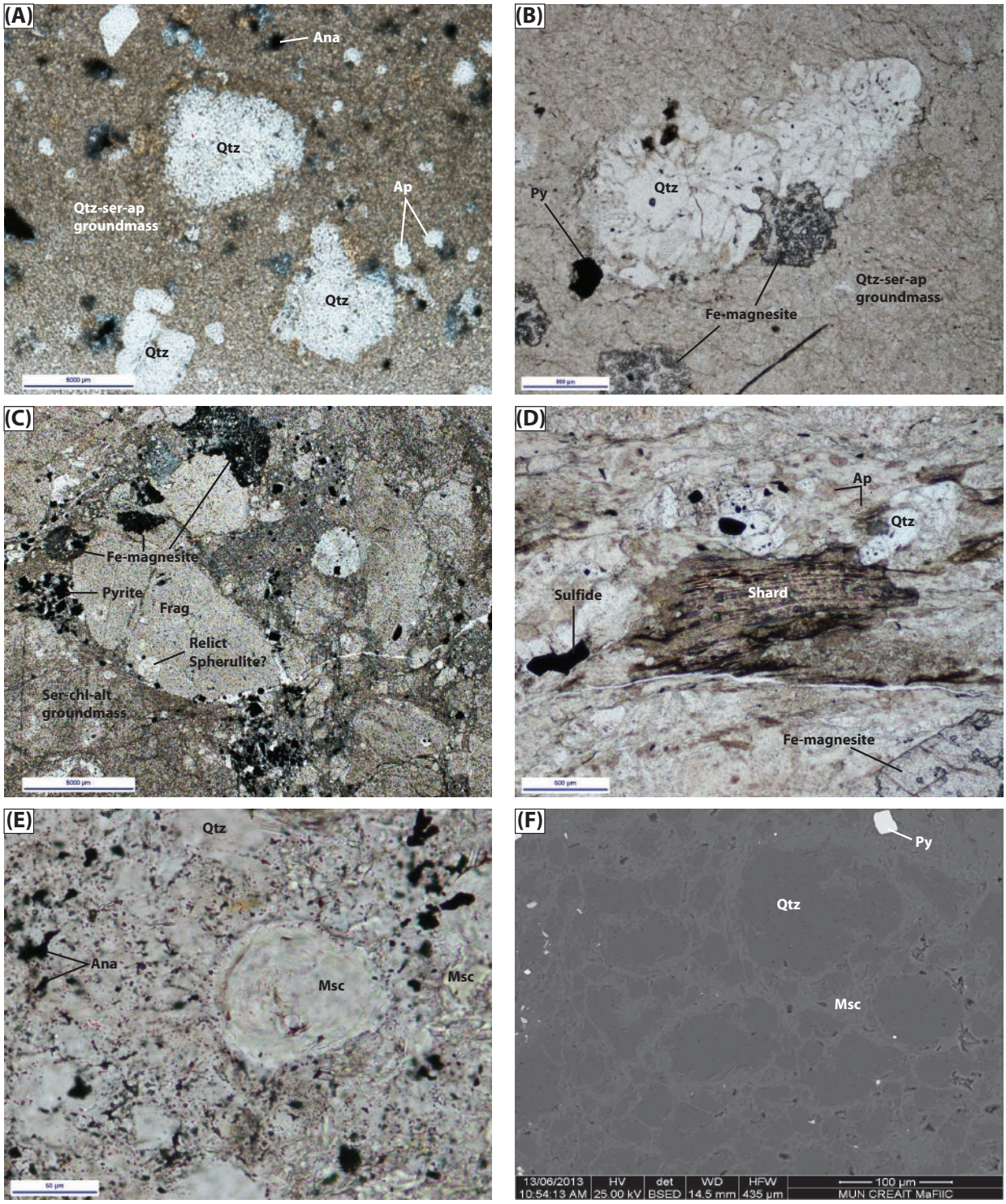

FIG. 10. Microscopic textures and weak alteration preserved in host rocks from the Boundary VMS deposit. (A) Hanging-wall quartz-phyric rhyolite flow with resorbed quartz within a clay altered groundmass. (B) Spherulitic quartz associated with ferromagnesite and quartz clots within a groundmass altered to quartz and sericite within hanging-wall rhyolite flow. (C) Footwall lapilli tuff with rounded rhyolitic fragments that contain relict spherulites hosted within a matrix of sericite-chlorite altered ash with pyrite and ferromagnesite clots. (D) Relict shard of glass with trains of Fe-oxides marking potential original flow bands in a matrix with quartz, sulfide, apatite, and clots of ferromagnesite within a footwall lapilli tuff. (E) Relict perlitic texture within a clast containing spherulitic muscovite with quartz, anatase, and muscovite within a footwall lapilli tuff. (F) Scanning electron microscope (SEM) image of relict perlite within a clast from footwall lapilli tuff containing rounded quartz surrounded by muscovite. Images A-E were taken in transmitted, plane-polarized light. Image (F) is a backscatter electron image. Abbreviations: alt = altered, Ana = anatase, Ap = apatite, Chl = chlorite, Frag = fragment, Msc = muscovite, Py = pyrite, Qtz = quartz, Ser = sericite.

converge, presumably near synvolcanic structures, and have a core of massive sulfide that, together with the bedding-parallel sheets, have a broad tree branch-like morphology (Figs. 5–8).

The mineralization consists of a variety of facies, including the following (Fig. 10): (1) stringer sulfides occurring within abundant clasts and in the matrix to clasts, (2) clast-rich massive sulfides, (3) massive pyritic sulfides with chalcopyrite stringers, (4) chalcopyrite- and sphalerite-rich massive sulfides, and (5) bedded sulfides. Stringer sulfides consist of fine-grained to granular pyrite and lesser chalcopyrite and sphalerite that occurs as ~10 to 20 vol % of the rock, forming the matrix to rhyolite lapilli (Fig. 11A), or surrounding the jigsaw-fit fragments in rhyolite flows (Fig. 9E, F). These stringers grade into clast-rich massive sulfide that consists predominantly of pyrite, sphalerite, and chalcopyrite with abundant, variably altered clasts of rhyolite (Fig. 11B, C). The clasts range from aphyric rhyolite lapilli (Fig. 11A), angular rhyolite fragments (Fig. 11B), to larger rounded rhyolitic fragments (Fig. 11C). Massive sulfide contains up to 90 to 95 vol % sulfide with varying proportions of pyrite, sphalerite, and chalcopyrite, and includes pyrite with stringers of sphalerite and chalcopyrite, and chalcopyrite with sphalerite and minor pyrite (Fig. 11D–F). Within the massive sulfides are abundant fragments of altered rhyolite (Fig. 11A–C). Bedded sulfides consist of laminated pyrite with lesser sphalerite and chalcopyrite that have mm- to cm-scale bands of sulfide (Fig. 11F).

Alteration: Within the Boundary deposit, altered rocks consist predominantly of chlorite and quartz-sericite of varying intensity with locally abundant dolomite ("chaotic carbonate") and Fe-carbonate (ferromagnesite). The type and extent of alteration vary between the footwall and hanging-wall lithofacies.

In the footwall, all alteration types are present going from unaltered to weakly altered ~100 m from mineralization to intensely altered proximal (i.e., within 10 m) to mineralization. In shallow holes (i.e., <100 m), rocks are rarely unaltered; however, in deeper holes the rocks are relatively fresh and display only minor quartz alteration (e.g., App. Fig. A2). The footwall lapilli tuff change becomes increasingly altered proximal to mineralization going from rocks that are relatively fresh, to quartz-sericite, to quartz-sericite-chlorite, to intense chlorite locally with chaotic carbonate near mineralization (Figs. 5–9). Clasts in moderately altered lapilli tuff have concentric alteration patterns with fresh cores surrounded by rims of quartz and sericite; the matrix of ash between the clasts is commonly replaced by chlorite (e.g., Fig. 11C). In strongly altered samples the clasts have similar concentric zonation but with chlorite-altered rims and quartz-sericite–altered cores within a matrix completely replaced by chlorite (Fig. 11A, C). In progressively altered rocks, the clasts and ash are entirely replaced by black chlorite with stringer sulfides; locally, the rock contains chaotic carbonate consisting of spheres and dendrites of dolomite that overprint, but are cogenetic with, chlorite (Fig. 11G).

Petrography and scanning electron microscopic (SEM) imaging of footwall alteration illustrates that weakly altered hanging-wall and footwall rocks have mostly sericite with lesser chlorite and carbonate alteration (Figs. 10A, B; 13A, B). Sericite-altered rocks exhibit an entire replacement of matrix and clasts by sericite, anatase, and locally apatite that exhibits a spherulitic texture (Figs. 10, 13; App. Fig. A3). More intensely altered chlorite-rich samples exhibit a near-complete replacement of the rocks by chlorite (Fig. 11G), with sulfide, carbonates, and anatase (Figs. 10, 13; App. Fig. A3). Both chlorite and sericite are associated with xenotime and monazite, particularly near carbonate (App. Fig. A3).

Unlike many VMS systems, the hanging wall to the Boundary deposit exhibits considerable alteration dominated by patchy to pervasive quartz-sericite, with only minor patchy chlorite (Figs. 9, 10). The rhyolite flows are typically white with flow-banded and massive zones having moderate to strong quartz-sericite alteration, whereas the ash-rich zones exhibit chlorite alteration (Figs. 9, 10). In some cases, the flow-banded zones also contain fine-grained Fe-oxides distributed parallel to the flow banding (Fig. 9A). Disseminated pyrite-(chalcopyrite-sphalerite) grains occur within the rhyolite flows as well.

Iron-rich carbonate alteration is also present throughout the Boundary deposit (and the entire Tally Pond Group) and occurs as mm-scale spots that overprint all other alteration types (Figs. 9, 10; App. Fig. A3). We interpret this as a late VMS-related hydrothermal alteration (e.g., Zaw and Large, 1992), or a much younger overprint related to Silurian(?) regional metamorphism (e.g., van Staal, 2007). Petrography and SEM identification suggest this carbonate is ferromagnesite and is distinct from the dolomite associated with chaotic carbonate alteration.

The footwall and hanging-wall alteration are spatially very distinctive. Moderate to intense quartz-sericite and minor to moderate chlorite alteration are broadly conformable to stratigraphy in both the footwall and hanging wall (Figs. 6–9; see also Lithogeochemistry below). Generally, the quartz-sericite and chlorite alteration parallel the sulfide lenses, with the former extending up to 10 m vertically into the hanging wall (total extent is uncertain due to erosion of the hanging wall), whereas the chlorite alteration extends less than 2 to 3 m into the hanging wall. Similarly, quartz-sericite typically extends up to ~100 m, whereas chlorite is typically ~10 m or less into the footwall. Very intense chlorite alteration does occur in discrete zones within the Boundary deposit, predominantly in the North zone and to a lesser extent in the South and Southeast zones (Figs. 6–9). Notably, the intense chlorite zones cross-cut stratigraphy and have both parallel and pipe-like (i.e., discordant form; e.g., Figs. 5–8). It is interpreted that these chloritic feeder pipes mark synvolcanic structures that controlled fluid flow within the deposit and fed the conformable, replacement-style alteration and mineralization.

Lithogeochemistry

Samples used for lithogeochemistry come from two representative drill holes from the North zone (BD99-108 and BD99-131) that represent the typical hydrothermal alteration styles in the Boundary deposit. Samples were collected every ~5 m in both the hanging wall and footwall so as to provide downhole profiles of alteration, and to constrain the primary chemostratigraphy of the host rocks to mineralization. Samples were analyzed at Activation Laboratories Inc., after being crushed and pulverized in mild steel. Analyses were obtained for major, trace, and REEs using a fusion pre-preparation,

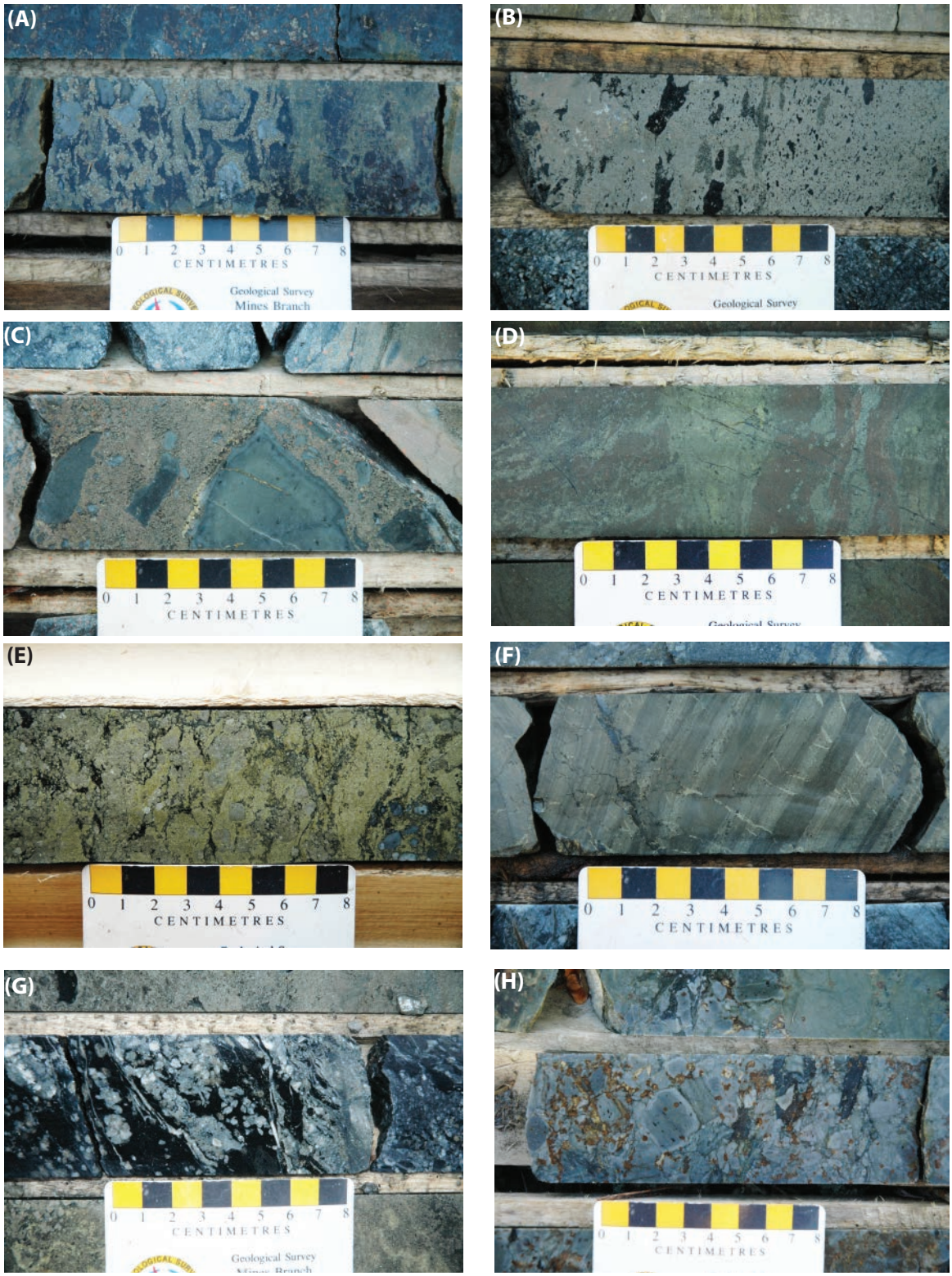

FIG. 11. Mineralization and alteration from the Boundary deposit. (A) Stringers of pyrite in between variably quartz-, sericite-, and chlorite-altered rhyolite lapilli. (B) Clast-rich massive sulfide with pyritic sulfides with small to variably angular chlorite-altered rhyolite fragments. (C) Sphalerite-rich massive sulfides with larger rounded, concentrically altered rhyolite fragments. (D) Massive pyrite- and chalcopyrite-rich sulfides with lesser pyrite and chlorite-altered gangue. (E) Bedded pyritic sulfides. (F) Chlorite-altered rhyolite with spheres and dendrites of dolomite, termed chaotic carbonate by previous workers (Squires et al., 2001). (G) Weakly quartz-altered rhyolite lapilli tuff to lapilli tuff with abundant, late ferromagnesite spots overprinting both the clasts and matrix of the sample. (H) Weakly quartz altered rhyolite lapillistone to lapilli tuff with abundant, late Fe-carbonate spots overprinting both the clasts and matrix of the sample.

$HF\text{-}HNO_3$ dissolution, and a combination of inductively coupled plasma-emission spectroscopy (ICP-ES) and inductively coupled plasma-mass spectrometry (ICP-MS). Mercury was determined by cold vapor-atomic absorption spectroscopy (CV-AAS); CO_2 was analyzed by infrared spectroscopy (IRS). Precision and accuracy of data reported by Actlabs have been quantified previously by Piercey and Colpron (2009). Lithogeochemical data are presented in Table 1.

Given the intense alteration of the rocks at the Boundary deposit, most major elements (except Al_2O_3 and TiO_2) and many trace elements, including the base metals, volatile metals, and the low field strength elements (LFSE), are considered mobile (e.g., Spitz and Darling, 1978; Saeki and Date, 1980; Jenner, 1996; Large et al., 2001b). In contrast, except under extreme conditions, the high field strength elements (HFSE) and REE (except Eu) are considered immobile (e.g., MacLean, 1990; MacLean and Barrett, 1993; Barrett and MacLean, 1999), except in cases of very intense alteration (e.g., Campbell et al., 1984) or the presence of key complexing ions (e.g., Bau and Dulski, 1995). The presence of monazite and xenotime, along with carbonate in the rocks, suggests the potential for REE and HFSE mobility (e.g., Taylor and Fryer, 1983; Murphy and Hynes, 1986). It must have been very local (i.e., hand specimen scale), as the HFSE, REE, Al_2O_3, and TiO_2 behave coherently regardless of alteration facies, suggesting they have been effectively immobile on the hand specimen scale during alteration and metamorphism. Based on these relationships, the mobile major elements, metals, and LFSE provide significant insight into the alteration and mineralization processes, whereas the HFSE, REE, Al_2O_3, and TiO_2 provide information on the primary chemostratigraphic and petrological attributes of the rocks.

Mobile element systematics

Rocks from the Boundary deposits are strongly altered with samples from both the footwall and hanging wall having very strong Na_2O depletions (Na_2O <0.5 wt %) and Spitz-Darling index (Al_2O_3/Na_2O) values >30 (Fig. 13A). The majority of

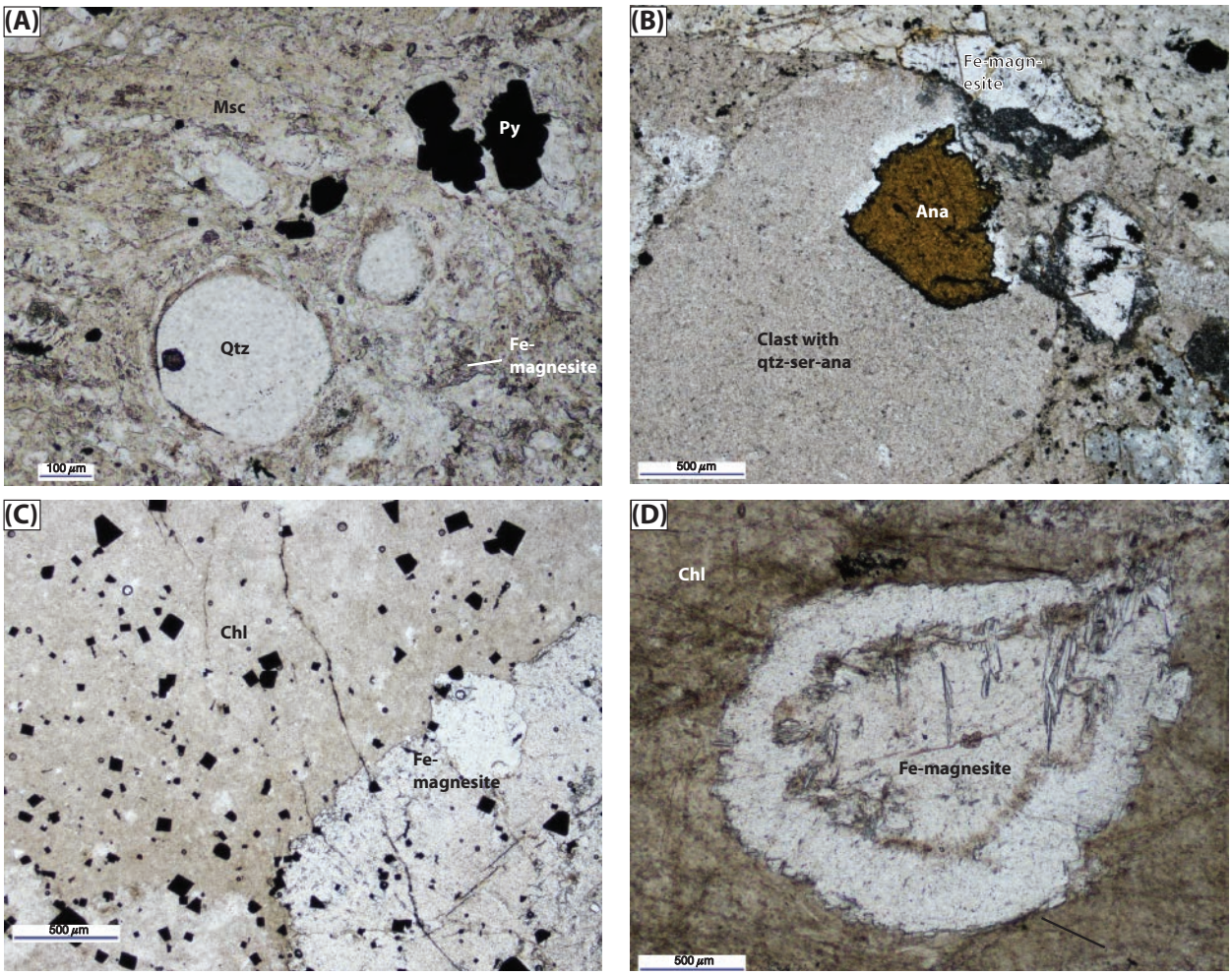

Fig. 12. Photomicrographs of footwall alteration at the Boundary deposit. A) muscovite(sericite)-quartz–Fe-magnesite alteration of the matrix of felsic tuff with pyrite crystals. B) Rounded rhyolite grain in lapilli tuff replaced by quartz-sericite-chlorite with anatase on the grain edge and surrounded by Fe-magnesite. C) Pervasive chlorite alteration of ash in rhyolitic lapilli tuff with pyrite grains and Fe-magnesite spots nearby. Fragment in the lower right has sericite-quartz alteration. D) Chaotic carbonate alteration with a subrounded grain of dolomite in the center of the figure surrounded by pervasive chlorite alteration of the matrix, and wisps of more fibrous chlorite within the dolomite grain. All images in plane-polarized light. Abbreviations: alt = altered, Ana = anatase, Chl = chlorite, Msc = muscovite, Qtz = quartz.

TABLE 1. Whole-Rock Lithogeochemical Data for Rhyolitic Rocks from the Boundary Deposit

Sample	BD99-131,7.37	BD99-131,17.53	BD99-131,24.2	BD99-131,28.36	BD99-131,33.86	BD99-131,38.5	BD99-131,45.2
Drill hole	BD99-131	BD99-131	BD99-131	BD99-131	BD99-131	BD99-131	BD99-131
Depth (m)	7.37	17.53	24.2	28.36	33.86	38.5	45.2
Rock type	Rhyolite	Rhyolite	Rhyolite	Rhyolite	Rhyolite	Lapilli tuff	Lapilli tuff
Subtype	Quartz phyric, massive	Quartz phyric, massive	Quartz phyric, massive	Quartz phyric, massive	Quartz phyric, massive	Aphyric, rhyo with minor ash	Aphyric, rhyo with minor ash
HW or FW	HW	HW	HW	HW	HW	FW	FW
Alteration	Fe-carb-ser	Fe-carb-ser	Quartz-chlorite-Fe-carb	Quartz-chlorite-Fe-carb	Quartz-Ser-Fe-carb	Quartz-Fe-carb-chlorite	Quarz-sericite-Fe-carb (minor)
SiO_2 (wt %)	70.95	72.93	67.85	73.89	77.83	62.29	75.47
Al_2O_3	10.97	11.61	12.22	10.54	9.59	13.72	11.06
Fe_2O_3(T)	6.14	3.41	3.11	4.30	2.66	6.39	3.28
MnO	0.15	0.16	0.13	0.10	0.10	0.19	0.05
MgO	3.14	2.42	2.28	2.66	3.27	5.54	1.82
CaO	0.27	0.12	0.06	0.07	0.06	0.24	0.09
Na_2O	0.32	0.31	0.27	0.21	0.25	0.24	0.23
K_2O	2.52	3.09	3.34	2.65	2.19	3.03	3.08
TiO_2	0.16	0.14	0.15	0.14	0.11	0.48	0.16
P_2O_5	0.01	0.02	0.02	<0.01	0.03	0.06	0.02
LOI	5.59	4.91	4.69	4.73	3.92	7.17	3.92
Total	100.20	99.11	94.13	99.29	100.00	99.35	99.18
CO_2 (wt %)	2.62	2.64	2.12	1.46	1.65	2.83	1.03
Hg (ppb)	8	102	2.5	5	9	137	481
S (wt %)	1.8	0.83	0.99	2.13	0.35	1.78	1.76
Sc (ppm)	10	10	11	9	8	22	11
Be	1	1	1	1	1	2	1
V	11	<5	<5	5	7	143	6
Cr	<20	<20	30	<20	30	30	<20
Co	4	1	<1	1	<1	12	3
Ni	<20	<20	<20	<20	<20	<20	<20
Cu	5	50	110	5	20	10	360
Zn	120	780	40	60	110	860	2,990
Ga	16	15	16	13	14	20	15
Ge	0.7	<0.5	<0.5	0.6	<0.5	0.6	<0.5
As	19	24	40	28	16	79	36
Rb	51	62	63	53	45	63	60
Sr	12	11	13	9	10	14	12
Y	52	36.9	48.7	39.7	36	39	44
Zr	173	148	164	161	114	136	169
Nb	6.9	5.1	5.7	6.3	3.7	5.4	6.2
Mo	<2	<2	<2	<2	<2	<2	2
Ag	<0.5	<0.5	<0.5	<0.5	<0.5	<0.5	<0.5
In	<0.1	0.1	<0.1	<0.1	<0.1	<0.1	<0.1
Sn	1	1	5	2	2	1	1
Sb	<0.2	0.5	3	<0.2	15.2	<0.2	<0.2
Cs	2	1.9	1.6	1.9	1.3	2.7	1.7
Ba	976	1,137	1,219	1,101	771	836	767
Th	5.18	5.33	5.39	4.86	4.14	3.65	5.03
U	1.76	1.31	1.49	1.53	1.44	1.38	1.56
La	18.8	17.8	17.8	19.7	13.1	15.4	19.8
Ce	41.7	39.9	39.5	43.6	30	34.7	44.8
Pr	5.11	4.49	4.44	5.09	3.4	4.23	5.35
Nd	20.9	18.8	18.5	19.8	14.6	17.2	21.4
Sm	5.05	4.77	4.87	4.68	3.87	4.23	5.17
Eu	0.764	0.74	0.719	0.747	0.73	1.32	1.33
Gd	6.42	5.12	5.26	5.56	4.46	5.25	6.02
Tb	1.24	0.92	0.99	1.03	0.84	0.97	1.11
Dy	8.07	5.69	6.49	6.46	5.29	6.15	6.99
Ho	1.69	1.21	1.46	1.35	1.14	1.27	1.48
Er	5.25	4.04	4.93	4.22	3.8	3.96	4.57
Tm	0.826	0.649	0.806	0.673	0.601	0.614	0.713
Yb	5.43	4.27	5.26	4.31	3.85	3.89	4.67
Lu	0.848	0.612	0.776	0.668	0.578	0.613	0.736
Hf	4.7	4	4.1	4.2	2.9	3.5	4.4
Ta	0.33	0.29	0.3	0.31	0.21	0.24	0.31
W	1.2	1	1.3	0.8	0.8	2.8	1
Tl	0.33	0.54	0.61	0.31	0.48	0.39	0.36
Pb	6	33	14	6	62	33	37
Bi	<0.1	0.9	0.6	0.1	0.9	0.6	0.2

TABLE 1. *(Cont.)*

Sample	BD99-131,52.7	BD99-131, 59.42	BD99-108, 7.8	BD99-108,14.2	BD99-108,17.15	BD99-108,19.9	BD99-108,22.5
Drill hole	BD99-131	BD99-131	BD99-109	BD99-109	BD99-109	BD99-109	BD99-109
Depth	52.7	59.42	7.8	14.2	17.15	19.9	22.5
Rock type	Lapilli tuff	Lapilli tuff	Rhyolite breccia	Rhyolite	Lapilli tuff	Lapilli tuff	Lapilli tuff
Subtype	Aphyric, rhyo with minor ash	Aphyric, rhyo with minor ash	Quartz phyrric	Quartz phyrric, mostly massive	Aphyric, rhyo with minor ash	Aphyric, rhyo with minor ash	Aphyric, rhyo with minor ash
HW or FW	FW	FW	HW	HW	FW	FW	FW
Alteration	Quartz-pyrite	Quartz-chlorite-Fe-carb	Quartz-chlorite-Fe-carb	Quartz-chlorite-Fe-carb	Quartz-sericite	Quartz-sericite	Quartz-sericite-chlorite
SiO_2 (wt %)	79.55	73.09	76.25	68.47	68.10	71.12	67.60
Al_2O_3	8.42	11.48	8.62	12.22	11.03	11.44	12.05
Fe_2O_3(T)	3.64	3.37	5.75	3.48	7.15	4.77	6.34
MnO	0.09	0.08	0.10	0.45	0.08	0.06	0.09
MgO	1.95	2.67	1.18	3.75	1.16	1.43	1.87
CaO	0.55	0.05	0.48	0.61	0.16	0.06	0.12
Na_2O	0.17	0.27	0.21	0.22	0.27	0.29	0.21
K_2O	2.14	2.78	2.45	3.18	3.21	3.37	3.54
TiO_2	0.12	0.17	0.11	0.14	0.17	0.18	0.18
P_2O_5	<0.01	0.03	0.02	0.02	0.02	<0.01	0.01
LOI	4.33	4.19	5.22	6.07	6.20	5.11	6.49
Total	101.00	98.18	100.40	98.59	97.53	97.84	98.50
CO_2 (wt %)	1.26	1.25	1.34	3.74	1.05	1.38	2.06
Hg (ppb)	336	14	619	34	781	500	580
S (wt %)	2.36	1.04	4.7	0.75	6.27	3.34	4.49
Sc (ppm)	10	12	7	10	11	11	12
Be	1	1	1	1	1	1	1
V	23	<5	<5	6	11	5	7
Cr	<20	30	<20	20	<20	20	<20
Co	3	<1	<1	<1	1	1	<1
Ni	<20	<20	<20	<20	<20	<20	<20
Cu	80	270	310	5	120	110	60
Zn	1,800	80	5,110	350	6,330	3,670	4,390
Ga	11	16	12	16	20	17	22
Ge	<0.5	<0.5	<0.5	0.9	<0.5	<0.5	0.8
As	47	23	273	13	610	165	81
Rb	44	56	50	69	67	65	70
Sr	14	9	12	26	14	11	12
Y	27.6	44.7	33	52.6	39.6	42.5	48.2
Zr	111	154	116	188	142	145	185
Nb	3	5.6	4.1	6.7	5.4	4.8	6.8
Mo	<2	3	<2	<2	<2	<2	<2
Ag	<0.5	<0.5	2.7	<0.5	6	3.8	1.3
In	<0.1	<0.1	0.2	<0.1	<0.1	0.2	0.2
Sn	1	1	6	1	13	7	5
Sb	3.4	3.1	11.9	0.4	15.5	12.7	3.7
Cs	1.2	1.8	1.3	1.6	1.7	1.6	2.7
Ba	554	739	1,909	1,699	3,058	3,058	3,051
Th	3.88	5.29	4.15	5.38	5.01	4.82	5.31
U	1.4	1.47	1.21	1.86	2.63	1.9	1.98
La	10.8	19.2	15.3	21.3	19.8	17.1	21.4
Ce	24.9	42.2	33.2	46.3	42.9	37.6	48
Pr	2.79	4.72	3.58	5.56	4.82	4.21	5.79
Nd	11.9	19.9	14.9	21.3	20	17.7	21.8
Sm	3.24	5.06	3.8	5.35	5	4.62	5.51
Eu	0.848	0.95	0.938	1.17	2.1	1.03	1.29
Gd	3.64	5.39	4.11	6.62	5.31	5.21	6.61
Tb	0.68	1.01	0.77	1.27	0.95	0.97	1.22
Dy	4.34	6.64	4.88	8.13	6.01	6.22	7.57
Ho	0.95	1.41	1.05	1.69	1.31	1.35	1.59
Er	3.14	4.68	3.5	5.22	4.31	4.42	5.02
Tm	0.51	0.75	0.565	0.817	0.686	0.715	0.777
Yb	3.28	4.85	3.62	5.44	4.42	4.66	5.04
Lu	0.469	0.711	0.527	0.842	0.662	0.68	0.79
Hf	2.8	3.9	2.9	4.8	3.6	3.4	4.8
Ta	0.19	0.29	0.23	0.31	0.3	0.29	0.36
W	0.9	2.3	1.2	1.1	1.8	1.4	1.7
Tl	0.41	0.54	0.65	1.26	2.49	1.29	0.76
Pb	24	30	3,610	228	3,530	3,120	1,110
Bi	5.1	1.3	0.4	<0.1	1.4	0.6	<0.1

TABLE 1. *(Cont.)*

Sample	BD99-108,27.3	BD99-108,30.3	BD99-108,33.7	BD99-108,35.7	BD99-108,38.64	BD99-108,42.5
Drill hole	BD99-109	BD99-109	BD99-109	BD99-109	BD99-109	BD99-109
Depth	27.3	30.3	33.7	35.7	38.64	42.5
Rock type	Lapilli tuff	Lapilli tuff	Lapilli tuff	Lapilli tuff	Lapilli tuff	Lapilli tuff
Subtype	Aphyric, rhyo with minor ash	Aphyric, rhyo with minor ash	Aphyric, rhyo with minor ash	Aphyric, rhyo with minor ash	Aphyric, rhyo with minor ash	Aphyric, rhyo with minor ash
HW or FW	FW	FW	FW	FW	FW	FW
Alteration	Chaotic carbonate, chlorite, pyrite	Chaotic carbonate, chlorite, pyrite	Cpy-py-chlorite	Chl-py	Chlorite	Quartz-carbonate
SiO_2 (wt %)	12.12	15.90	19.60	41.61	49.73	58.17
Al_2O_3	4.26	10.71	15.45	15.31	14.66	9.01
Fe_2O_3(T)	12.11	12.15	36.69	19.18	11.09	13.45
MnO	0.39	0.40	0.11	0.10	0.13	0.16
MgO	11.91	16.22	11.28	12.05	15.01	7.60
CaO	18.04	16.08	0.08	0.07	0.19	0.08
Na_2O	0.12	0.28	0.15	0.11	0.14	0.19
K_2O	0.95	1.35	0.22	0.18	0.32	0.38
TiO_2	0.09	0.17	0.24	0.20	0.22	0.14
P_2O_5	0.15	0.08	0.02	<0.01	0.03	0.04
LOI	17.95	24.79	16.46	9.72	9.39	8.00
Total	78.09	98.12	100.30	98.55	100.90	97.21
CO_2 (wt %)	28.60	24.60	2.93	2.52	2.72	3.38
Hg (ppb)	3,460	506	160	574	10	54
S (wt %)	10.8	3.14	14.5	3.32	0.17	3.59
Sc (ppm)	5	13	14	9	15	9
Be	<1	1	<1	<1	<1	<1
V	16	15	22	<5	6	6
Cr	<20	<20	<20	<20	<20	<20
Co	<1	<1	62	5	3	19
Ni	<20	<20	<20	<20	<20	<20
Cu	570	80	8,840	1,960	160	10,000
Zn	10,000	3,500	380	3,710	260	190
Ga	14	25	41	28	21	17
Ge	<0.5	<0.5	1.1	0.9	0.9	0.7
As	181	12	177	11	<5	13
Rb	19	29	5	4	7	9
Sr	120	117	10	7	10	12
Y	18.6	37	83.3	68.7	63.5	33.5
Zr	67	133	229	249	254	116
Nb	2.5	4.5	7.9	8.6	8.8	5
Mo	<2	2	25	3	3	4
Ag	2.7	0.7	2	<0.5	<0.5	1.4
In	0.9	0.4	0.8	0.2	<0.1	0.2
Sn	9	7	1	4	1	3
Sb	7.9	7.3	4.6	<0.2	1.8	4.4
Cs	0.5	1.8	1.3	0.7	1.7	0.6
Ba	483	657	96	132	127	132
Th	2.15	4.36	8.02	7.32	6.72	4.07
U	3.21	12.9	15	3.98	2.68	1.33
La	6.82	21.5	29.8	26.8	21.4	8.32
Ce	15.4	45.1	66.2	60.5	46.4	18.3
Pr	1.78	5.07	6.84	7.4	5.46	2.04
Nd	7.9	21.5	30.1	29.9	21.4	9.38
Sm	2.13	5.54	8.09	7.29	5.08	2.68
Eu	1.36	2.23	1.92	1.2	0.99	0.529
Gd	2.49	5.55	9.84	8.73	6.92	3.75
Tb	0.42	0.93	1.93	1.65	1.4	0.74
Dy	2.62	5.72	12.7	10.7	9.49	4.96
Ho	0.57	1.22	2.77	2.23	2.06	1.1
Er	1.83	3.85	8.77	6.87	6.45	3.44
Tm	0.3	0.613	1.33	1.07	1.01	0.541
Yb	1.99	4.02	8.38	7.11	6.73	3.57
Lu	0.297	0.59	1.23	1.1	1.05	0.542
Hf	1.7	3.5	6.3	6.5	6.5	3.2
Ta	0.11	0.23	0.5	0.39	0.43	0.22
W	2.5	3.1	16.2	3	2.8	7.8
Tl	0.025	0.025	0.31	0.08	0.11	0.1
Pb	3,200	183	142	8	13	32
Bi	4.7	0.3	14.7	1.1	0.2	4.5

Abbreviations: Fe-carb = Fe-carbonate, FW = footwall, HW= hanging wall, rhyo = rhyolite, Ser = sericite

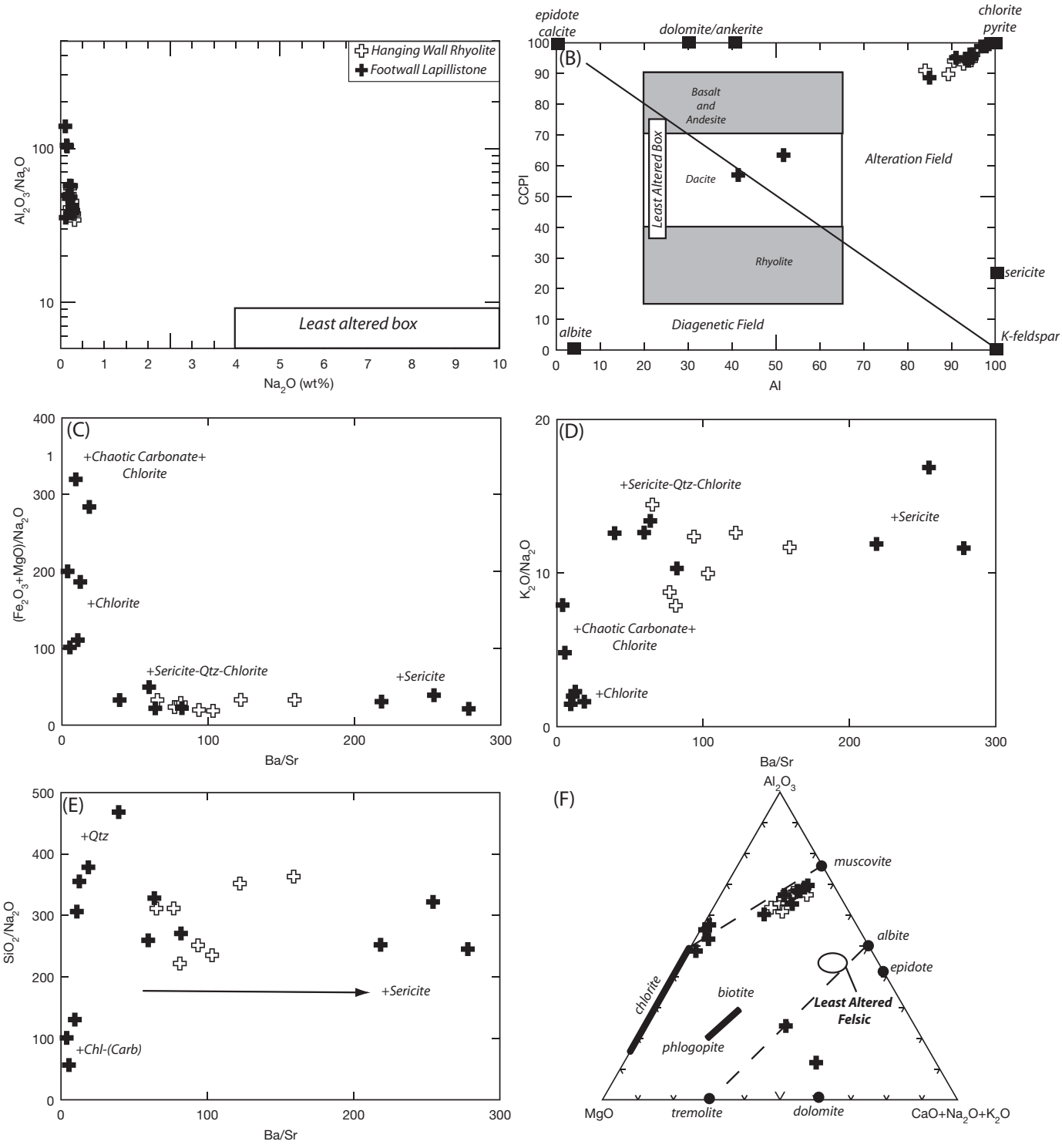

FIG. 13. Mobile element plots for rhyolitic rocks from the Boundary VMS deposit. (A) Spitz-Darling (Spitz and Darling, 1978) index versus Na_2O (diagram after Ruks et al., 2006). (B) Alteration box plot with the chlorite-carbonate pyrite index (CCPI) against the Hashimoto alteration index (AI; Saeki and Date, 1980; Date et al., 1983; Large et al., 2001b). (C) Chlorite-carbonate alteration monitor ($(Fe_2O + MgO)/Na_2O$) vs. Ba/Sr index. (D) Sericite alteration monitor (K_2O/Na_2O) vs. Ba/Sr. (E) Quartz alteration monitor (SiO_2/Na_2O) against Ba/Sr. (F) MgO-Al_2O_3-(CaO + Na_2O + K_2O) plot with various mineral nodes (diagram after MacDonald et al., 1996).

rocks have high Hashimoto index [100 × MgO + K_2O/(MgO + K_2O + CaO + Na_2O)] and chlorite-carbonate-pyrite index [CCPI = 100 × MgO + Fe_2O_3/(MgO + Fe_2O_3 + CaO + Na_2O)] values, with most samples plotting close to the chlorite-pyrite node of the diagram, except two chaotic carbonate-altered samples that trend toward the field for least-altered dacite (Fig. 13B).

Samples spatially associated with mineralization in the Tally Pond belt have historically been known for high Ba/Sr ratios, with the exception of those showing very intense chlorite and/or chaotic carbonate alteration (Collins, 1989). Notably, there is a distinctive distribution of Ba/Sr ratios for the Boundary samples, with most samples having Ba/Sr >25, with a subset that has low Ba/Sr (Fig. 13). The low-Ba/Sr group displays high (Fe_2O_3 + MgO)/Na_2O ratios, consistent with chlorite, chaotic carbonate, and/or sulfide alteration (Fig. 13A), whereas the high-Ba/Sr group is characterized by high K_2O/Na_2O, consistent with sericite alteration (Fig. 13C, D). The low-Ba/Sr group shows contrasting SiO_2/Na_2O ratios with some low-Ba/Sr samples having low SiO_2/Na_2O ratios (chlorite ± carbonate alteration) and others showing high SiO_2/Na_2O ratios (chlorite-quartz alteration); the high-Ba/Sr samples have moderate SiO_2/Na_2O ratios consistent with sericite-chlorite-quartz alteration (Fig. 13E). A similar distribution of data exists in MgO-Al_2O_3-alkali space where most samples plot close to the sericite node, trending toward chlorite. The chlorite-rich samples lie close to the chlorite node; the carbonate-altered samples trend toward the MgO-alkali axis (Fig. 13F). Unlike many other VMS deposits (e.g., Large et al., 2001a), rocks from the Boundary deposit lack anomalously high Tl and Sb contents (Fig. 14A). They do, however, have elevated Hg contents, and very high ratios of Hg/Na_2O and Ba/Sr (Collins index), a feature previously designated by Collins (1989) as the "Duck Pond alteration signature" (Fig. 14B). The chaotic-carbonate–altered samples are also characterized by very high CO_2/Na_2O ratios coupled with high (CaO + MgO)/Na_2O ratios (Fig. 14C).

Downhole profiles of drill holes BD99-108 and BD99-131 for key elements, alteration indexes, and metals are shown in Figures 15 and 16. Hole BD99-108 contains a significant footwall intersection and shows typical footwall alteration signatures with depletions in Na_2O, high alteration indices, and

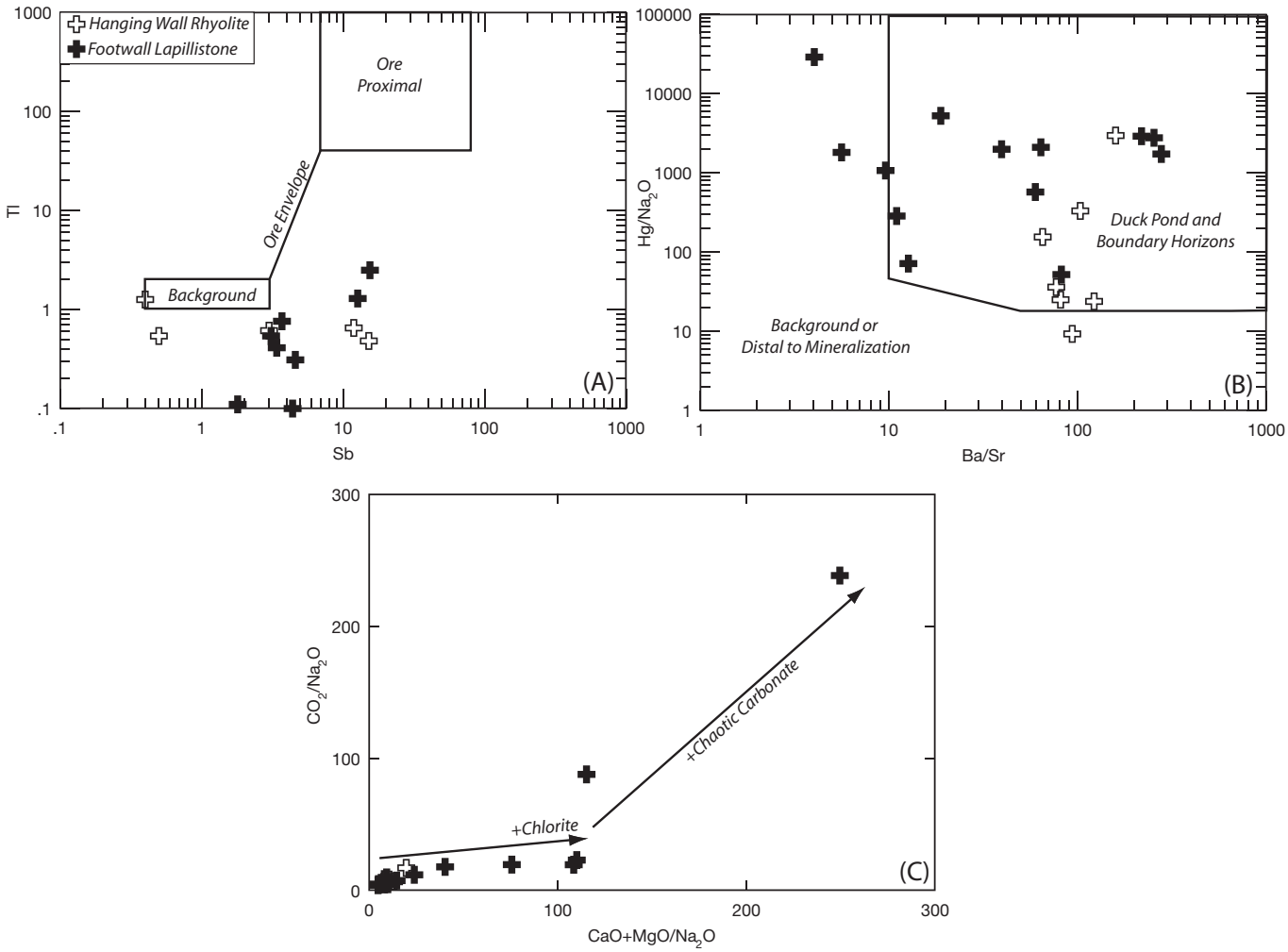

FIG. 14. Volatile element plots for rhyolitic rocks from the Boundary VMS deposit. (A) Tl-Sb plot of Large et al. (Large et al., 2001a). (B) Hg/Na_2O-Ba/Sr plot of the "Duck Pond index" of Collins (1989). (C) Carbonate monitor diagram of CO_2/Na_2O vs. (CaO + MgO)/Na_2O.

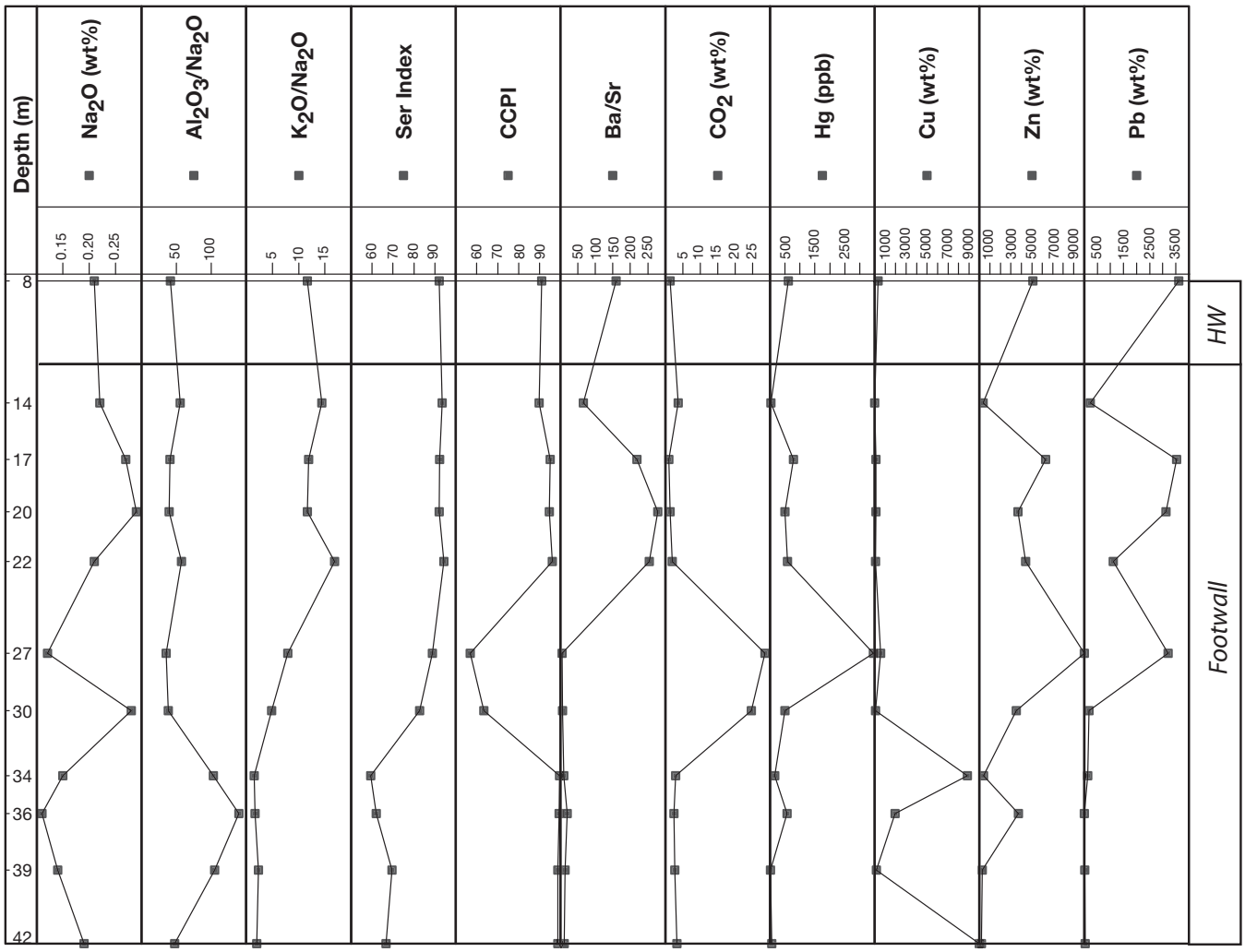

FIG. 15. Downhole profiles of key element and alteration index values for drill hole BD99-108.

anomalously high base metal contents. Notably, both the sericite index (K_2O/Na_2O) and Ba/Sr ratios decrease with depth, corresponding to increases in CO_2 and Cu contents and higher Al_2O_3/Na_2O ratios, indicative of chlorite-chaotic carbonate alteration. Hole BD99-131 contains similar footwall alteration signatures, but also has a significant hanging-wall intersection (Fig. 16). The hanging wall in BD99-131 also has low Na_2O contents (<0.5 wt %), high Al_2O_3/Na_2O (>30), high K_2O/Na_2O and Ba/Sr ratios, and anomalously high base metals, Hg, and CO_2 consistent with significant hanging-wall alteration.

Immobile element systematics

Plots of data for immobile elements are shown in Figures 17 and 18. Despite variable alteration, the Zr/TiO_2 and Nb/Y ratios of the Boundary samples, except one chaotic-carbonate–altered sample, exhibit a tight clustering with rhyolitic petrological affinities and subalkalic Nb/Y ratios. Significantly, there is no discernable difference between the footwall and hanging wall (Fig. 17A). Most samples have Zr/Y ratios of 2.8 to 4.5, typical of transitional series rocks (Fig. 17B), and low Nb/Y ratios that plot within the volcanic arc field (Fig. 17C), suggesting formation in an arc or re-melted arc crust (e.g., Lentz, 1998). Upper crust–normalized La/Sm ratios are <1, implying derivation from crust that was more juvenile than normal upper continental crust (Fig. 17D). The primitive mantle-normalized signatures of these samples are slightly LREE-enriched with flat HREE, and negative Nb, Ti, and Eu anomalies, accompanied by very low contents of compatible elements (Al, Sc, V; Fig. 18), typical of fractionated rhyolitic rocks that formed in an arc environment or by re-melting of arc basement (e.g., Piercey, 2011, and references therein).

Discussion and Summary

Evidence for subseafloor replacement

Although subseafloor replacement has been advocated as a fundamental mechanism in the formation of many VMS deposits, finding unequivocal evidence of this process in ancient deposits is very difficult. The Boundary deposit is exceptionally well preserved and contains textures and features common to subseafloor replacement-style VMS deposits. Doyle and Allen (2003) proposed five criteria that are indicative of subseafloor replacement in VMS deposits: (1) enclosure of mineralized horizons by rapidly emplaced volcanic or

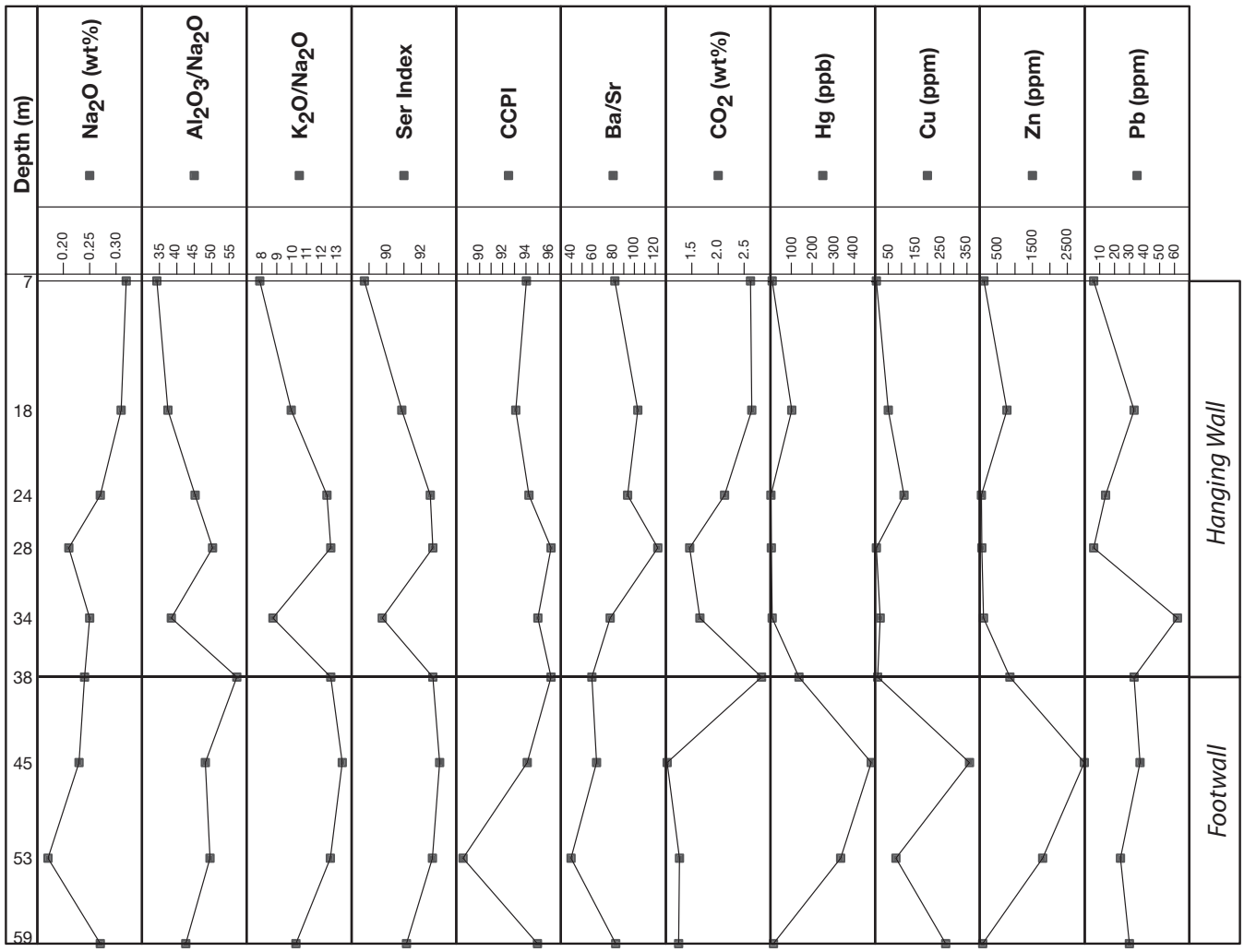

FIG. 16. Downhole profiles of key element and alteration index values for drill hole BD99-131.

sedimentary facies, (2) relicts of host facies within the mineral deposit, (3) replacement fronts between the deposit and host lithofacies, (4) discordance of the deposit to bedding, and (5) strong hanging-wall alteration without an abrupt break in intensity. Criteria 1 to 3 are considered diagnostic, whereas criteria 4 and 5 are supportive but non-unique to replacement (Doyle and Allen, 2003). Most of these criteria are present in the Boundary deposit.

Although the rate of emplacement of the rocks at Boundary cannot be determined, the poorly sorted, nonbedded rhyolitic lapilli tuff that form the footwall can be reasonably assumed to record rapid deposition as mass flows (e.g., McPhie et al., 1993; McPhie and Allen, 2003). Capping of these lapilli tuff by flow-banded lobe and lobe and breccia facies rhyolites that are hydrothermally altered is also consistent with rapid emplacement as lava flows, synchronous with high-temperature hydrothermal alteration (see below). The textural and stratigraphic relationships at Boundary provide evidence for a subseafloor replacement origin. The ubiquitous presence of clasts having textures and alteration identical to the surrounding footwall lapilli tuff (Figs. 9, 11; criteria 2), together with the occurrence of multiple sulfide lenses at different stratigraphic levels beneath the rhyolite cap (Figs. 5–8; criteria 3) are diagnostic of subseafloor replacement.

Discordant mineralization is also present at Boundary. In many drill holes in the North zone (e.g., BD99-113), cross-cutting chlorite alteration has a pipe-like structure (e.g., Fig. 5B) that transitions laterally into alteration parallel to stratigraphy; this is particularly well developed in porous footwall volcaniclastic rocks at multiple stratigraphic levels (Figs. 5–8). Furthermore, the alteration is pervasive in hanging-wall rocks with very little change in intensity relative to that present in the footwall (Figs. 15, 16). In particular, there is strong Na_2O depletion, elevated alteration index values, and anomalously high base and volatile metals in the hanging-wall rhyolite flows (Figs. 13–16), features that suggest that these rhyolites had already been deposited prior to sulfide mineralization (i.e., during replacement), or were emplaced shortly thereafter while the hydrothermal system was still active.

Formation of the Boundary deposit was likely enhanced and ultimately related to the significant permeability contrast between the relatively impermeable hanging-wall rhyolite flows and more porous footwall volcaniclastic rocks (Fig. 19). Metalliferous fluid flow was controlled by synvolcanic

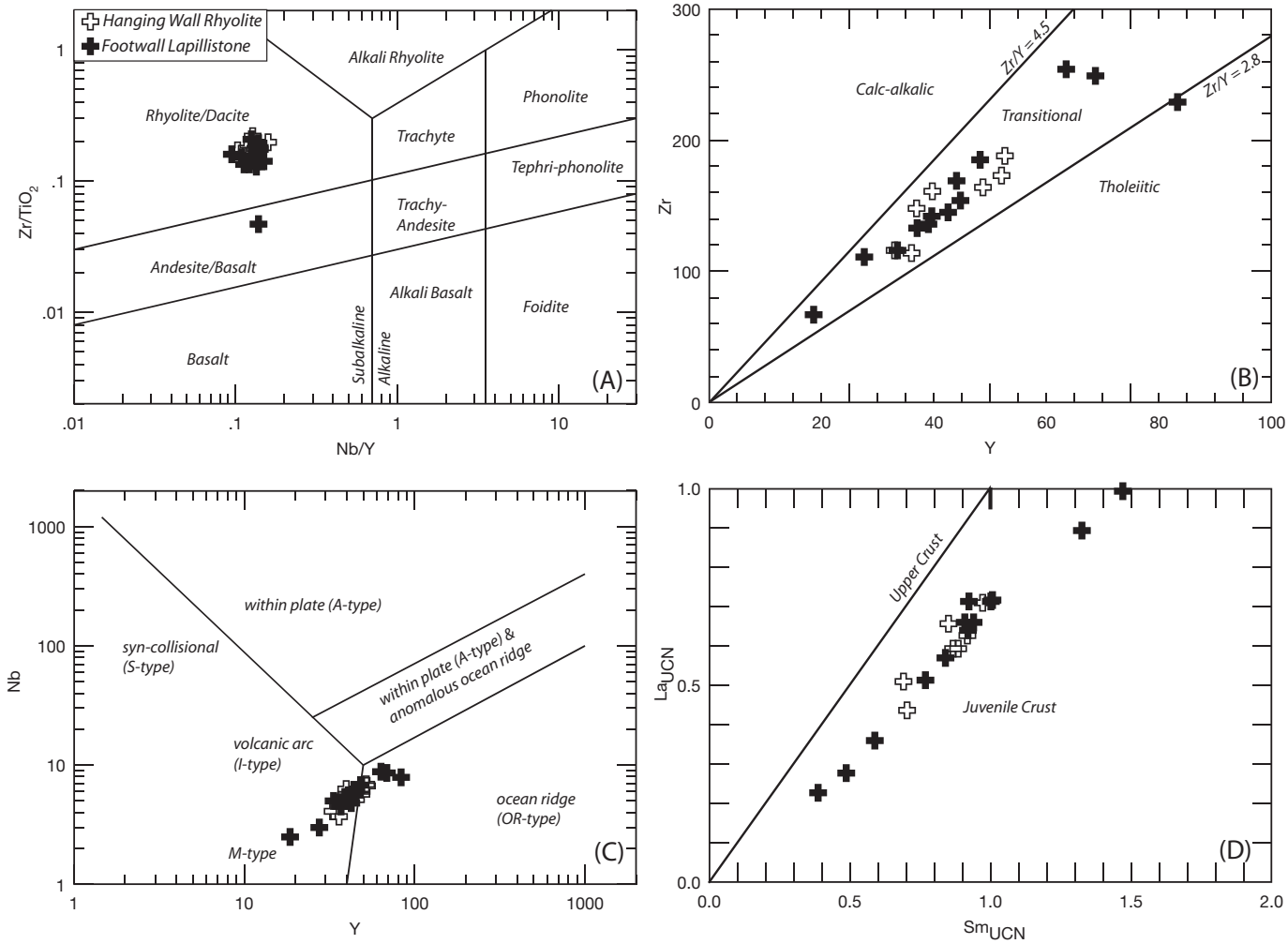

FIG. 17. Immobile element plots for rhyolitic rocks from the Boundary VMS deposit. (A) Modified Winchester and Floyd (1977) Zr/TiO_2-Nb/Y discrimination diagram for rock classification (from Pearce, 1996). (B) Zr-Y diagram for discriminating magma affinity (from Ross and Bedard, 2009). (C) Nb-Y tectonic discrimination diagram (from Pearce et al., 1984). (D) Upper-crust normalized La-Sm diagram (upper crust values from McLennan, 2001; from Piercey and Colpron, 2009)

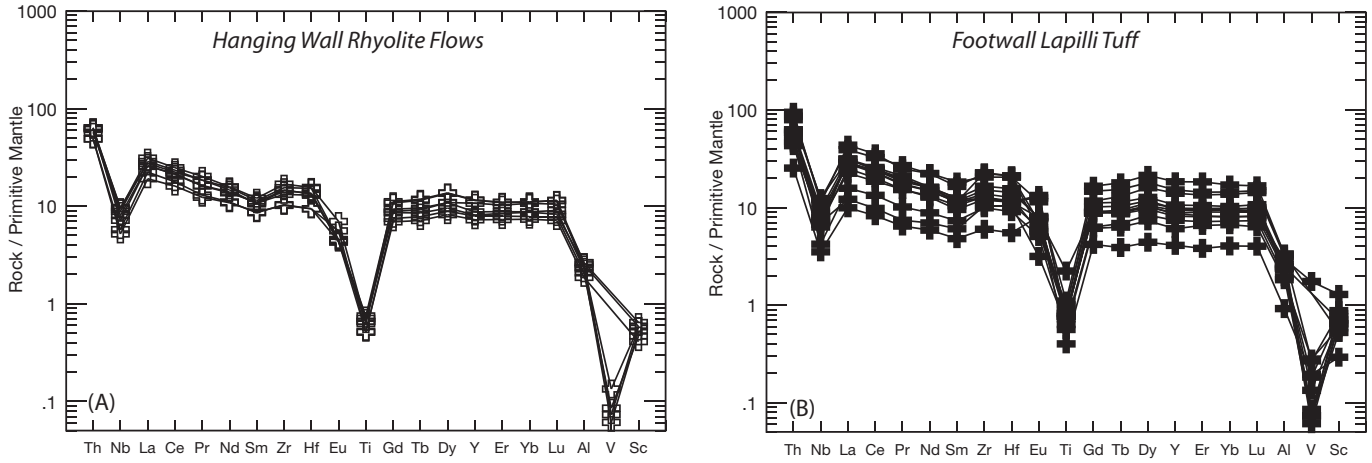

FIG. 18. Primitive mantle normalized multi-element plots (primitive mantle values from Sun and McDonough, 1989) of rhyolitic rocks from the Boundary VMS deposit. (A) Hanging-wall rhyolitic flows. (B) Footwall lapilli tuff.

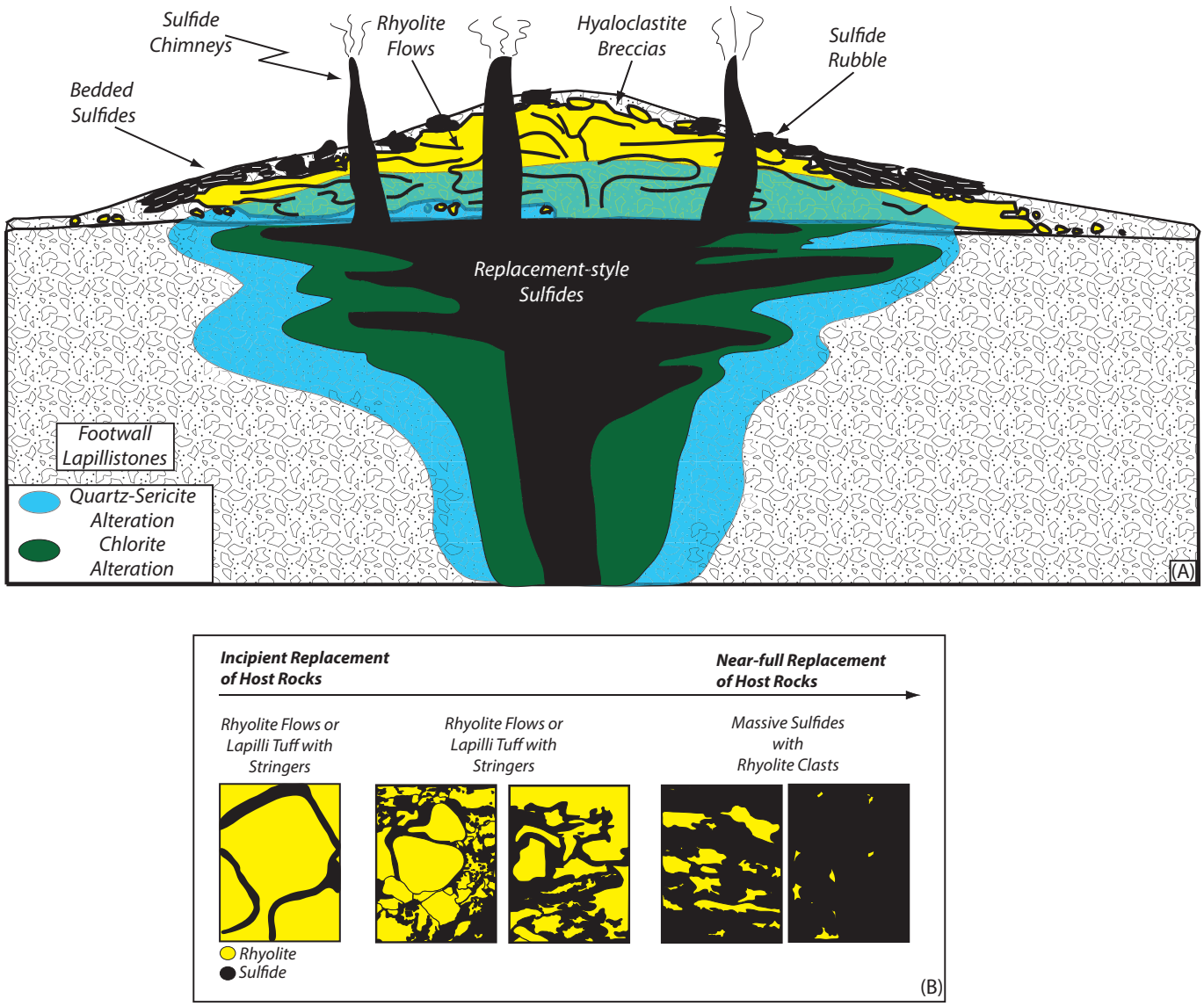

FIG. 19. (A) Potential reconstructed environment of formation for the Boundary deposit. The deposit formed at the boundary between hanging-wall rhyolite lobe and breccia facies rhyolite, likely domal in form, and the footwall of rhyolitic lapilli tuff. The vast majority of sulfide in the deposit likely formed by replacement of footwall lapilli tuff as a result of fluids cooling, mixing with seawater and with porewater at a permeability boundary between more impermeable hanging-wall rhyolite flows and more permeable footwall lapilli tuff. This resulted in a massive core of sulfide and a tree-like structure of sulfides replacing the bounding permeable lapilli tuff. This was also responsible for the shape of the alteration halo broadly paralleling stratigraphy in both the footwall and hanging wall. Notably, there are bedded sulfides in the deposit, suggesting that part of the deposit must have exhaled on the seafloor and was subsequently eroded. (B) Schematic of the progressive replacement of rhyolite breccias toward mostly massive sulfide with rhyolite clasts. This schematic illustrates the potential range of textures found in the massive sulfides and the potential mechanism for their formation. Diagram influenced and constructed based on diagrams in Gibson et al. (1999) and McPhie et al. (1993)

structures and rose through the relatively permeable footwall lapilli tuff, and upon encountering the impermeable hanging-wall rhyolites, cooled, mixed with ambient seawater and porewater in the volcaniclastic rocks, and deposited sulfides in a subseafloor setting. The multiple sulfide zones present in the deposit also suggest that variable permeable zones existed in the footwall volcaniclastic rocks that promoted the deposition of multiple mineralized horizons. Permeability boundaries resulted in the progressive replacement of the host rocks ranging from rhyolite with sulfide stringers, to sulfide-rich rhyolite, to massive sulfide with abundant rhyolite clasts, to predominantly massive sulfide with rare clasts (Fig. 19).

Subseafloor mineralization would have been accompanied by zoned alteration typical of VMS systems in which sericite then chlorite form with increasing proximity to sulfides (e.g., Riverin and Hodgson, 1980; Gemmell and Large, 1992; Franklin et al., 2005; Gibson, 2005). In addition to a classic, discordant alteration zone (e.g., Fig. 5B; Gemmell and Large, 1992), the Boundary deposit also has alteration that parallels stratigraphy and extends into the hanging wall (Figs. 5–8, 19),

features very common to subseafloor replacement-style VMS (see also Galley et al., 1993). Moreover, the presence of a cap rock during sulfide mineralization resulted in extensive alteration of hanging-wall strata and is consistent with a replacement style origin (e.g., Figs. 15, 16, 19); however, hanging-wall alteration is not diagnostic and could represent continuation of hydrothermal fluid flow after deposit formation.

Despite significant evidence for subseafloor replacement, at least part of the Boundary deposit must have breached the surface and formed in the seafloor environment (Fig. 19). The laminated and bedded sulfides present at Boundary (Fig. 12), although much less abundant than the replacement-style sulfides, are consistent with mineralization on the seafloor and may have formed either from chimney collapse and subsequent deposition, and/or by tectonic uplift of the deposit (during rifting?), erosion, and deposition (Fig. 19). Some of these laminated, semi-massive sulfides also could be replacements of fine-grained tuff.

Tectonic environment of formation

The regional setting of mineralization in the Tally Pond Group has been the focus of numerous studies. Dunning et al. (1991) argued that the group was the product of arc volcanism potentially within a thickened arc or on continental crust. More recently, U-Pb geochronology and Nd isotope data suggest that some of the felsic rocks in the Tally Pond Group have Neoproterozoic zircon inheritance and Proterozoic depleted mantle model ages (Rogers et al., 2006; McNicoll et al., 2010). Furthermore, Pb isotope data from the Tally Pond belt range from relatively primitive to evolved signatures (Swinden and Thorpe, 1984; Pollock, 2004); however, some of the "evolved" galena samples used for Pb isotope analysis have questionable links to VMS systems, and may represent younger "orogenic" mineralization (i.e., crosscutting Zn-Pb carbonate veins; S.J. Piercey, unpub. data). Nevertheless, given the above data, Rogers et al. (2006) and Zagorevski et al. (2010) proposed that the Tally Pond Group formed in an arc sequence as part of the Penobscot-Victoria arc, in a peri-Gondwanan setting along the margin of Ganderia (Fig. 20). McNicoll et al. (2010) also suggested formation within a peri-Gondwanan continental arc along Ganderia (Fig. 20).

Immobile element geochemical signatures of felsic volcanic rocks from the Boundary deposit are consistent with formation in a predominantly continental arc environment. These rocks have low HFSE contents and negative Nb-Ti anomalies (the arc signature) on primitive mantle-normalized plots

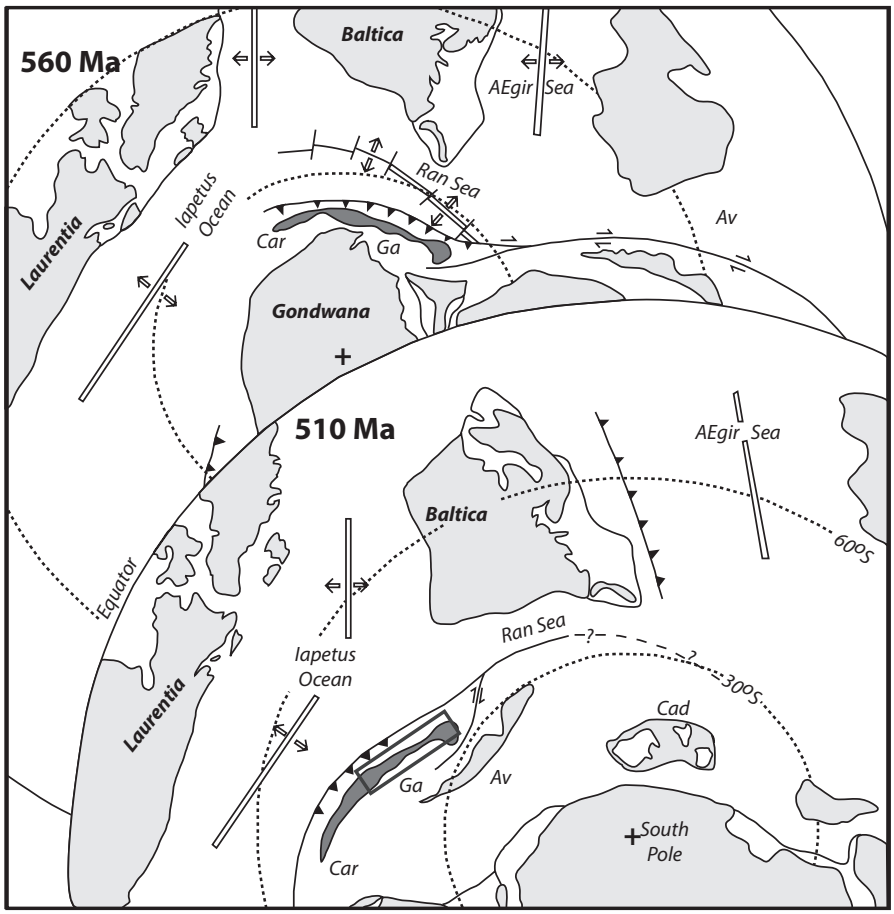

FIG. 20. Neoproterozoic to middle Cambrian paleogeography of the Iapetus. The Boundary deposit likely formed in southern latitudes in a peri-Gondwanan setting along the edge of Ganderia, likely within a rifted arc along this margin. The location of the potential environment of the Boundary deposit outlined in the blue box. Abbreviations in the figure: A = Avalonia, Cad = Cadomia, Car = Carolina Terrane, F = Florida, Ga = Ganderia (darker gray shading). Diagram modified from Rogers et al. (2006).

(Figs. 17, 18). Notably, however, such arc signatures in felsic rocks can form in a number of ways, including inheritance from their source region (e.g., remelting an arc source; Morris et al., 2000), contamination by continental crust (e.g., Piercey et al., 2001; Piercey, 2011), fractionation of Nb- and Ti-rich phases (e.g., Green and Pearson, 1987; Ryerson and Watson, 1987), and/or melting of hydrated crust where Ti phases are stable (e.g., Schmitt and Vazquez, 2006; Shukuno et al., 2006). Although the results presented here are consistent with formation in a continental arc environment, the geochemical signatures of the Boundary host rocks are not a unique indicator of this setting.

Other inconsistencies exist with a model involving formation in a typical continental arc. Firstly, there are abundant rocks having "primitive" geochemical signatures, including island arc tholeiites (Dunning et al., 1991) and VMS-related galena with unradiogenic Pb isotope ratios (e.g., Swinden and Thorpe, 1984). Similarly, the felsic rocks have upper-crust–normalized La/Sm values that are <1, indicative of formation from crustal sources more juvenile than typical upper continental crust (Fig. 17D). Secondly, the belt is distinctly bimodal and comprises a generally older, mafic-dominated package and a younger, more felsic-dominated package that hosts the sulfide mineralization. This pattern is atypical of continental arcs that generally show a continuous fractionation sequence from basalt, through andesite, dacite, and rhyolite, and in which andesitic rocks predominate (e.g., Arculus, 1994; Lentz, 1998; Swinden, 1996). Thirdly, the volcanic facies present at Boundary and other VMS deposits of the Tally Pond belt are consistent with formation in extensional synvolcanic structures, and not in a compressional environment typical of an Andean-type continental arc.

Zagorevski et al. (2010) argued that the Penobscot-Victoria arc was under extension during its Cambrian-Ordovician history that included periodic rifting (Fig. 20). This type of model explains most of the inconsistencies outlined above and provides the best potential tectonic environment for the Boundary deposit: a continental(?) rifted arc. An extending, continental arc rift setting would produce the volcanic facies observed within the Boundary deposit, as these facies are deposited preferentially in extensional grabens that form during arc extension (Gibson et al., 1999; Gibson, 2005). An extending arc would also explain the petrological and isotopic attributes of the volcanic rocks. Firstly, rifting of an arc leads to upwelling of asthenospheric mantle, basaltic underplating of the crust, and melting of the base of arc crust and/or continental crust, resulting in the formation of rhyolitic rocks having geochemical signatures variably influenced by crustal components (e.g., Piercey, 2011). For magmas that had sufficient residence time in the middle to upper crust, crust-mantle interaction could have occurred with older continental crust or slightly older arc crust, resulting in the evolved Nd isotope signatures and inherited zircons present in some rocks from the Tally Pond Group (Rogers et al., 2006; McNicoll et al., 2010; Zagorevski et al., 2010). Extension, however, would also allow some magma to be generated and emplaced with shorter crustal residence times, thereby decreasing the "crustal" signature found in some samples (e.g., Fig. 17D) and producing rhyolitic rocks with variable crustal versus mantle contributions during their genesis (Lentz, 1998; Zagorevski et al., 2010).

Variability in the crustal petrological signatures found in the felsic (and mafic) host rocks in the Boundary deposit area would also be recorded in Pb isotope ratios of the sulfide minerals of the deposits. In particular, given that Pb in VMS deposits is derived primarily by the leaching of the substrate beneath the deposits (Franklin et al., 2005), any Pb isotope variability in the volcanic basement will also be present in associated VMS mineralization, which is the case for VMS deposits of the Tally Pond Group (Swinden and Thorpe, 1984; Pollock, 2004).

In summary, although data for the Boundary deposit and Tally Pond Group are broadly consistent with formation in a continental arc, the data are more consistent with the deposits having formed within a rifted arc environment along the edge of Ganderia in the Iapetus Ocean (Fig. 20).

Acknowledgments

Financial and logistical support for this project was provided by Aur Resources Ltd. (and subsequently Teck Resources Ltd.) and a Natural Sciences and Engineering Research Council of Canada (NSERC) Discovery Grant to Piercey. Logistical support was also provided by John Hinchey and the Geological Survey of Newfoundland and Labrador. Piercey is also funded by the NSERC-Altius Industrial Research Chair at Memorial University, which is supported by NSERC, Altius Resources Inc., and the Research and Development Corporation of Newfoundland and Labrador. Numerous discussions with staff at the Duck Pond mine, particularly Isobel Wolfson, Darren Hennessey, and Bernie Macneil, and ongoing discussions and collaborative research with John Hinchey of the Geological Survey of Newfoundland and Labrador on VMS deposits of central Newfoundland, are gratefully acknowledged. *Economic Geology* reviewers Bruce Gemmell and Dave Lentz, and Associate Editor John Slack are thanked for their reviews and suggestions, which have greatly improved the manuscript.

REFERENCES

Arculus, R.J., 1994, Aspects of magma genesis in arcs: Lithos, v. 33, p. 189–208.

Bau, M., and Dulski, P., 1995, Comparative study of yttrium and rare-earth element behaviours in fluorine-rich hydrothermal fluids: Contributions to Mineralogy and Petrology, v. 119, p. 213–223.

Barrett, T.J., and MacLean, W. H., 1999, Volcanic sequences, lithogeochemistry, and hydrothermal alteration in some bimodal volcanic-associated massive sulfide systems, Reviews in Economic Geology, v. 8, p. 101–131.

Bradshaw, G.D., Rowins, S.M., Peter, J.M., and Taylor, B.E., 2008, Genesis of the Wolverine volcanic sediment-hosted massive sulfide deposit, Finlayson Lake district, Yukon, Canada: Mineralogical, mineral chemical, fluid inclusion, and sulfur isotope evidence: Economic Geology, v. 103, p. 35–60.

Campbell, I.H., Lesher, C.M., Coad, P., Franklin, J.M., Gorton, M.P., and Thurston, P.C., 1984, Rare-earth element mobility in alteration pipes below massive Cu-Zn sulfide deposits: Chemical Geology, v. 45, p. 181–202.

Collins, C.J., 1989, Report on lithogeochemical study of the Tally Pond Volcanics and associated alteration and mineralization: Unpublished Report for Noranda Exploration Company Limited (Assessment File 012A/1033 Newfoundland Department of Mines and Energy, Mineral Lands Division): St. John's, Newfoundland, 87 p.

Copeland, D.A., Toole, R.M., and Piercey, S.J., 2009, 10th year supplementary assessment report on soil sampling, linecutting, titan 24 geophysical surveying, diamond drilling and petrography, licence 8183M, South Tally Pond property, Rogerson Lake area, Newfoundland and Labrador, NTS 12A/10 and 12A/07: St. John's, NL, Canada, Newfoundland and Labrador Geological Survey Assessment File, 56 p.

Date, J., Watanabe, Y., and Saeki, Y., 1983, Zonal alteration around the Fukazawa Kuroko deposits, Akita Prefecture, northern Japan: Economic Geology Monograph 5, p. 365–386.

Doyle, M.G., and Allen, R.L., 2003, Subsea-floor replacement in volcanic-hosted massive sulfide deposits: Ore Geology Reviews, v. 23, p. 183–222.

Doyle, M.G., and Huston, D.L., 1999, The subseafloor replacement origin of the Ordovician Highway-Reward volcanic-associated massive sulfide deposit, Mount Windsor Subprovince, Australia: Economic Geology, v. 94, p. 825–844.

Dunning, G.R., and Krogh, T.E., 1985, Geochronology of ophiolites of the Newfoundland Appalachians: Canadian Journal of Earth Sciences, v. 22, p. 1659–1670.

Dunning, G.R., Kean, B.F., Thurlow, J.G., and Swinden, H.S., 1987, Geochronology of the Buchans, Roberts Arm, and Victoria Lake groups and Mansfield Cove Complex, Newfoundland: Canadian Journal of Earth Sciences, v. 24, p. 1175–1184.

Dunning, G.R., Swinden, H.S., Kean, B.F., Evans, D.T.W., and Jenner, G.A., 1991, A Cambrian island arc in Iapetus: Geochronology and geochemistry of the Lake Ambrose volcanic belt, Newfoundland Appalachians: Geological Magazine, v. 128, p. 1–17.

Evans, D.T.W., and Kean, B.F., 2002, The Victoria Lake Supergroup, central Newfoundland: Its definition, setting and volcanogenic massive sulfide mineralization: Newfoundland and Labrador Department of Mines and Energy, Geological Survey, Open File NFLD/2790, 68 p.

Evans, D.T.W., Kean, B.F., and Dunning, G.R., 1990, Geological studies, Victoria Lake Group, central Newfoundland: Current Research Report, Geological Survey Branch, Report 90-1, p. 131–144.

Fisher, R.V., 1966, Rocks composed of volcanic fragments and their classification: Earth-Science Reviews, v. 1, p. 287–298.

Franklin, J.M., Gibson, H.L., Galley, A.G., and Jonasson, I.R., 2005, Volcanogenic massive sulfide deposits: Economic Geology 100th Anniversary Volume, p. 523–560.

Galley, A.G., Bailes, A.H., and Kitzler, G., 1993, Geological setting and hydrothermal evolution of the Chisel Lake and North Chisel Zn-Pb-Cu-Ag-Au massive sulfide deposits, Snow Lake, Manitoba: Exploration and Mining Geology, v. 2, p. 271–295.

Galley, A.G., Watkinson, D.H., Jonasson, I.R., and Riverin, G., 1995, The subsea-floor formation of volcanic-hosted massive sulfide: Evidence from the Ansil deposit, Rouyn-Noranda, Canada: Economic Geology, v. 90, p. 2006–2017.

Gemmell, J.B., and Large, R.R., 1992, Stringer system and alteration zones underlying the Hellyer volcanic-hosted massive sulfide deposit, Tasmania, Australia: Economic Geology, v. 87, p. 620–649.

Gibson, H.L., 2005, Volcanic-hosted ore deposits, *in* Marti, J., and Ernst, G.G.J., eds., Volcanoes in the environment: New York, Cambridge University Press, p. 332–386.

Gibson, H.L., Morton, R.L., and Hudak, G.J., 1999, Submarine volcanic processes, deposits, and environments favorable for the location of volcanic-associated massive sulfide deposits, Reviews in Economic Geology, v. 8, p. 13–51.

Goodfellow, W.D., McCutcheon, S.R., and Peter, J.M., eds., 2003, Massive sulfide deposits of the Bathurst mining camp, New Brunswick, and northern Maine: Economic Geology Monograph 11, 930 p.

Green, T.H., and Pearson, N.J., 1987, An experimental study of Nb and Ta partitioning between Ti-rich minerals and silicate liquids at high pressure and temperature: Geochimica et Cosmochimica Acta, v. 51, p. 55–62.

Hannington, M.D., Barrie, C.T., and Bleeker, W., 1999, The giant Kidd Creek volcanogenic massive sulfide deposit, western Abitibi subprovince, Canada: Preface and introduction: Economic Geology Monograph 10, p. 1–30.

Hannington, M.D., de Ronde, C.E.J., and Petersen, S., 2005, Sea floor tectonics and submarine hydrothermal systems: Economic Geology 100th Anniversary Volume, p. 111–142.

Hibbard, J.P., van Staal, C.R., Rankin, D., and Williams, H., 2004, Lithotectonic map of the Appalachian orogen, Canada–United States of America: Geological Survey of Canada, Map 2096A, scale 1:500,000.

Hinchey, J.G., 2007, Volcanogenic massive sulfides of the southern Tulks volcanic belt, central Newfoundland: Preliminary findings and overview of styles and environments of mineralization, *in* Pereira, C.P.G., and Walsh, D.G., eds., Current Research Report 07-1: St. John's, Newfoundland, Geological Survey Branch, p. 117–143.

——2008, Volcanogenic massive sulfides of the northern Tulks volcanic belt, central Newfoundland: Preliminary findings, overview of deposit reclassifications, and mineralizing environments., *in* Pereira, C.P.G., and Walsh, D.G., eds., Current Research Report 08-01: St. John's, Newfoundland, Geological Survey Branch, p. 151–172.

——2011, The Tulks volcanic belt, Victoria Lake Supergroup, central Newfoundland: Geology, tectonic setting, and volcanogenic massive sulfide mineralization: St. John's, NL, Canada, Newfoundland and Labrador Department of Natural Resources, Geological Survey, Report 2011-02, 167 p.

Hinchey, J.G., and McNicoll, V., 2009, Tectonostratigraphic architecture and VMS mineralization of the southern Tulks volcanic belt: New insights from U-Pb geochronology and lithogeochemistry, *in* Pereira, C.P.G., and Walsh, D.G., eds., Current Research Report 09-01: St. John's, Newfoundland, Geological Survey Branch, p. 13–42.

Jenner, G.A., 1996, Trace element geochemistry of igneous rocks: Geochemical nomenclature and analytical geochemistry, *in* Wyman, D.A., ed., Trace Element Geochemistry of Volcanic Rocks: Applications for Massive Sulfide Exploration: Geological Association of Canada, Short Course Notes, v. 12, p. 51–77.

Jenner, G.A., Dunning, G.R., Malpas, J., Brown, M., and Brace, T., 1991, Bay of Islands and Little Port complexes, revisited: Age, geochemical and isotopic evidence confirm suprasubduction-zone origin: Canadian Journal of Earth Sciences, v. 28, p. 1635–1652.

Kean, B.F., and Evans, D.T.W., 1986, Metallogeny of the Tulks Hill Volcanics, Victoria Lake Group, central Newfoundland: Report—Government of Newfoundland and Labrador, Department of Mines and Energy, Mineral Development Division, v. 86-1, p. 51–57.

Kean, B.F., Evans, D.T.W., and Jenner, G.A., 1995, Geology and mineralization of the Lushs Bight Group: St. John's, Newfoundland, Geological Survey of Newfoundland and Labrador, Mineral Development Division, Report 95-05, 204 p.

Large, R.R., 1992, Australian volcanic-hosted massive sulfide deposits: Features, styles, and genetic models: Economic Geology, v. 87, p. 471–510.

Large, R.R., Allen, R.L., Blake, M.D., and Herrmann, W., 2001a, Hydrothermal alteration and volatile element haloes for the Rosebery K Lens volcanic-hosted massive sulfide deposit, western Tasmania: Economic Geology, v. 96, p. 1055–1072.

Large, R.R., Gemmell, J.B., Paulick, H., and Huston, D.L., 2001b, The alteration box plot: A simple approach to understanding the relationships between alteration mineralogy and lithogeochemistry associated with VHMS deposits: Economic Geology, v. 96, p. 957–971.

Lentz, D.R., 1998, Petrogenetic evolution of felsic volcanic sequences associated with Phanerozoic volcanic-hosted massive sulfide systems: The role of extensional geodynamics: Ore Geology Reviews, v. 12, p. 289–327.

MacDonald, R.W.J., Barrett, T.J., and Sherlock, R.L., 1996, Geology and lithogeochemistry at the Hidden Creek massive sulfide deposit, Anyox, west-central British Columbia: Exploration and Mining Geology, v. 5, p. 369–398.

MacLachlan, K., and Dunning, G., 1998a, U-Pb ages and tectono-magmatic evolution of Middle Ordovician volcanic rocks of the Wild Bight Group, Newfoundland Appalachians: Canadian Journal of Earth Sciences, v. 35, p. 998–1017.

——1998b, U-Pb ages and tectonomagmatic relationships to Early Ordovician low-Ti tholeiites, boninites, and related plutonic rocks in central Newfoundland, Canada: Contributions to Mineralogy and Petrology, v. 133, p. 235–258.

MacLean, W.H., 1990, Mass change calculations in altered rock series: Mineralium Deposita, v. 25, p. 44–49.

MacLean, W.H., and Barrett, T.J., 1993, Lithogeochemical techniques using immobile elements: Journal of Geochemical Exploration, v. 48, p. 109–133.

McLennan, S.M., 2001, Relationships between the trace element composition of sedimentary rocks and upper continental crust: Geochemistry, Geophysics, Geosystems, v. 2, Paper 2000GC000109.

McNicoll, V., Squires, G., Kerr, A., and Moore, P., 2010, The Duck Pond and Boundary Cu-Zn deposits, Newfoundland: New insights into the ages of host rocks and the timing of VHMS mineralization: Canadian Journal of Earth Sciences, v. 47, p. 1481–1506.

McPhie, J., and Allen, R.L., 2003, Submarine, silicic, syn-eruptive pyroclastic units in the Mount Read Volcanics, western Tasmania: Influence of vent setting and proximity on lithofacies characteristics, *in* White, J.D.L., Smellie, J.L., and Clague, D.A., eds., Explosive subaqueous volcanism: San Francisco, American Geophysical Union, Geophysical Monograph 140, p. 245–258.

McPhie, J., Doyle, M., and Allen, R.L., 1993, Volcanic textures: A guide to the interpretation of textures in volcanic rocks: Hobart, Australia, Centre for Ore Deposit and Exploration Studies, University of Tasmania, 198 p.

Moore, P.J., 2003, Stratigraphic implications for mineralization: Preliminary findings of a metallogenic investigation of the Tally Pond Volcanics, central Newfoundland, *in* Pereira, C.P.G., Walsh, D.G., and Kean, B.F., eds., Current Research Report 03-1: St. John's, Newfoundland, Geological Survey Branch, p. 241–257.

Morris, G.A., Larson, P.B., and Hooper, P.R., 2000, "Subduction style" magmatism in a non-subduction setting: The Colville igneous complex, NE Washington State, USA: Journal of Petrology, v. 41, p. 43–67.

Murphy, J.B., and Hynes, A.J., 1986, Contrasting secondary mobility of Ti, P, Zr, Nb, and Y in two metabasaltic suites in the Appalachians: Canadian Journal of Earth Sciences, v. 23, p. 1138–1144.

Pearce, J.A., 1996, A user's guide to basalt discrimination diagrams, *in* Wyman, D.A., ed., Trace element geochemistry of volcanic rocks: Applications for massive sulfide exploration: Geological Association of Canada, Short Course Notes, v. 12, p. 79–113.

Pearce, J.A., Harris, N.B.W., and Tindle, A.G., 1984, Trace element discrimination diagrams for the tectonic interpretation of granitic rocks: Journal of Petrology, v. 25, p. 956–983.

Piercey, S., 2011, The setting, style, and role of magmatism in the formation of volcanogenic massive sulfide deposits: Mineralium Deposita, v. 46, p. 449–471.

——2007, Volcanogenic massive sulfide (VMS) deposits of the Newfoundland Appalachians: An overview of their setting, classification, grade-tonnage data, and unresolved questions, *in* Pereira, C.P.G., and Walsh, D.G., eds., Current Research, Report 07-01: St. John's, Newfoundland, Geological Survey Branch, p. 169–178.

Piercey, S.J., and Colpron, M., 2009, Composition and provenance of the Snowcap assemblage, basement to the Yukon-Tanana terrane, northern Cordillera: Implications for Cordilleran crustal growth: Geosphere, v. 5, p. 439–464.

Piercey, S.J., Paradis, S., Murphy, D.C., and Mortensen, J.K., 2001, Geochemistry and paleotectonic setting of felsic volcanic rocks in the Finlayson Lake volcanic-hosted massive sulfide (VHMS) district, Yukon, Canada: Economic Geology, v. 96, p. 1877–1905.

Pollock, J., 2004, Geology and paletectonic history of the Tally Pond Group, Dunnage zone, Newfoundland Appalachians: An integrated geochemical, geochronological, metallogenic and isotopic study of a Cambrian island arc along the Peri-Gondwanan margin of Iapetus: Unpublished M.Sc. thesis, St. John's, Newfoundland, Memorial University, 420 p.

Riverin, G., and Hodgson, C.J., 1980, Wall-rock alteration at the Millenbach Cu-Zn mine, Noranda, Quebec: Economic Geology, v. 75, p. 424–444.

Rogers, N., and van Staal, C.R., 2002, Toward a Victoria Lake Supergroup: A provisional stratigraphic revision of the Red Indian to Victoria Lakes area, central Newfoundland: Current Research–Newfoundland, Geological Survey Branch, Report 02-1, p.185–195.

Rogers, N., van Staal, C.R., McNicoll, V., Pollock, J., Zagorevski, A., and Whalen, J., 2006, Neoproterozoic and Cambrian arc magmatism along the eastern margin of the Victoria Lake Supergroup: A remnant of Ganderian basement in central Newfoundland?: Precambrian Research, v. 147, p. 320–341.

Rogers, N., van Staal, C., Zagorevski, A., Skulski, T., Piercey, S.J., and McNicoll, V., 2007, Timing and tectonic setting of volcanogenic massive sulfide bearing terranes within the Central Mobile belt of the Canadian Appalachians, *in* Milkereit, B., ed., Proceedings of Exploration 07: Toronto, Fifth Decennial International Conference on Mineral Exploration, September 9-12, 2007, p. 1199–1205.

Ross, P.-S., and Bedard, J.H., 2009, Magmatic affinity of modern and ancient subalkaline volcanic rocks determined from trace-element discriminant diagrams: Canadian Journal of Earth Sciences, v. 46, p. 823–839.

Ruks, T.W., Piercey, S.J., Ryan, J.J., Villeneuve, M.E., and Creaser, R.A., 2006, Mid- to late Paleozoic K-feldspar augen granitoids of the Yukon-Tanana terrane, Yukon, Canada: Implications for crustal growth and tectonic evolution of the northern Cordillera: Geological Society of America Bulletin, v. 118, p. 1212–1231.

Ryerson, F.J., and Watson, E.B., 1987, Rutile saturation in magmas: Implications for the Ti-Nb-Ta depletion in island-arc basalts: Earth and Planetary Science Letters, v. 86, p. 225–239.

Saeki, Y., and Date, J., 1980, Computer application to the alteration data of the footwall dacite lava at the Ezuri Kuroko deposits, Akito Prefecture: Mining Geology, v. 30, p. 241–250.

Schmitt, A.K., and Vazquez, J.A., 2006, Alteration and remelting of nascent oceanic crust during continental rupture: Evidence from zircon geochemistry of rhyolites and xenoliths from the Salton Trough, California: Earth and Planetary Science Letters, v. 252, p. 260–274.

Shukuno, H., Tamura, Y., Tani, K., Chang, Q., Suzuki, T., and Fiske, R.S., 2006, Origin of silicic magmas and the compositional gap at Sumisu submarine caldera, Izu-Bonin arc, Japan: Journal of Volcanology and Geothermal Research, v. 156, p. 187–216.

Skulski, T., Castonguay, S., McNicoll, V.J., and van Staal, C., 2008, New constraints on the geology of Baie Berte Peninsula, Newfoundland; Part 1, Tectonostratigraphy of ophiolites and their volcanic cover [abs]: Geological Society of America Abstracts with Programs, v. 40, p. 28.

Skulski, T., Castonguay, S., McNicoll, V., van Staal, C., Kidd, W., Rogers, N., Morris, W., Ugalde, H., Slavinski, H., Spicer, W., Moussallam, Y., and Kerr, I., 2010, Tectonostratigraphy of the Baie Verte oceanic tract and its ophiolite cover sequence on the Baie Verte Peninsula: Current Research: Newfoundland and Labrador Department of Natural Resources, Geological Survey, Report 10-1, p. 315–225.

Spitz, G., and Darling, R., 1978, Major and minor element lithogeochemical anomalies surrounding the Louvem copper deposit, Val d'Or, Quebec: Canadian Journal of Earth Sciences, v. 15, p. 1161–1169.

Squires, G.C., and Moore, P.J., 2004, Volcanogenic massive sulfide environments of the Tally Pond Volcanics and adjacent area: Geological, lithogeochemical and geochronological results, *in* Pereira, C.P.G., Walsh, D.G., and Kean, B.F., eds., Current Research Report 04-1: St. John's, Newfoundland, Geological Survey Branch, p. 63–91.

Squires, G.C., MacKenzie, A.C., and MacInnis, D., 1991, Geology and genesis of the Duck Pond volcanogenic massive sulfide deposit, *in* Swinden, H.S., Evans, D.T.W., and Kean, B.F., eds., Metallogenic framework of base and precious metal deposits, central and western Newfoundland: Geological Survey of Canada Open File 2156, p. 56–64.

Squires, G.C., Brace, T.D., and Hussey, A.M., 2001, Newfoundland's polymetallic Duck Pond deposit: Earliest Iapetan VMS mineralization formed within a sub-seafloor, carbonate-rich alteration system, *in* Evans, D.T.W., and Kerr, A., eds., Geology and mineral deposits of the northern Dunnage zone, Newfoundland Appalachians: St. John's, Newfoundland, Geological Association of Canada-Mineralogical Association of Canada, Field Trip Guide A2, p. 167–187.

Sun, S.-s., and McDonough, W.F., 1989, Chemical and isotopic systematics of oceanic basalts: Implications for mantle composition and processes, *in* Saunders, A.D., and Norry, M.J., eds., Magmatism in the ocean basins: Geological Society Special Publication 42, p. 313–345.

Swinden, H.S., 1991, Paleotectonic settings of volcanogenic massive sulfide deposits in the Dunnage zone, Newfoundland Appalachians: Canadian Institute of Mining and Metallurgy Bulletin, v. 84, p. 59–89.

——1996, The application of volcanic geochemistry in the metallogeny of volcanic-hosted sulphide deposits in central Newfoundland, *in* Wyman, D.A., ed., Trace element geochemistry of volcanic rocks: Applications for massive sulfide exploration: Geological Association of Canada, Short Course Notes, v. 12, p. 329–358.

Swinden, H.S., and Thorpe, R.I., 1984, Variations in style of volcanism and massive sulfide deposition in Early to Middle Ordovician island-arc sequences of the Newfoundland Central Mobile belt: Economic Geology, v. 79, p. 1596–1619.

Swinden, H.S., Jenner, G.A., Kean, B.F., and Evans, D.T.W., 1989, Volcanic rock geochemistry as a guide for massive sulfide exploration in central Newfoundland: Newfoundland Department of Mines, Current Research Report 89-1, p. 201–219.

Taylor, R.P., and Fryer, B.J., 1983, Rare earth element lithogeochemistry of granitoid mineral deposits: Canadian Institute of Mining Bulletin, v. 76, p. 74–84.

Thurlow, J.G., 2010, Great mining camps of Canada 3: The history and geology of the Buchans mine, Newfoundland and Labrador: Geoscience Canada, v. 37, p. 145–173.

Van Staal, C.R., 2007, Pre-Carboniferous tectonic evolution and metallogeny of the Canadian Appalachians, *in* Goodfellow, W.D., ed., Mineral deposits of Canada: A synthesis of major deposit types, district metallogeny, the evolution of geological provinces, and exploration methods: Geological Association of Canada, Mineral Deposits Division Special Publication 5, p. 793–818.

Van Staal, C., and Barr, S.M., 2012, Lithospheric architecture and tectonic evolution of the Canadian Appalachians and associated Atlantic margin. Chapter 2, *in* Percival, J.A., Cook, F.A., and Clowes, R.M., eds., Tectonic styles in Canada: The LITHOPROBE perspective: Geological Association of Canada Special Paper 49, p. 41–96.

Van Staal, C.R., and Colman-Sadd, S.P., 1997, The Central Mobile belt of the northern Appalachians: Oxford Monographs on Geology and Geophysics, v. 35, p. 747–760.

Wagner, D.W., 1993, Volcanic stratigraphy and hydrothermal alteration associated with the Duck Pond and Boundary volcanogenic massive sulphide deposits, Central Newfoundland: Unpublished MSc. thesis, Ottawa, Ontario, Canada, Carleton University, 430 p.

White, J.D.L., and Houghton, B.F., 2006, Primary volcaniclastic rocks: Geology, v. 34, p. 677–680.

Williams, H., 1979, Appalachian orogen in Canada: Canadian Journal of Earth Sciences, v. 16, p. 792–807.

Williams, H., Colman-Sadd, S.P., and Swinden, H.S., 1988, Tectonostratigraphic subdivisions of central Newfoundland: Geological Survey of Canada, Current Research, Part B, Paper 88-1B, p. 91–98.

Winchester, J.A., and Floyd, P.A., 1977, Geochemical discrimination of different magma series and their differentiation products using immobile elements: Chemical Geology, v. 20, p. 325–343.

Zagorevski, A., van Staal, C.R., and McNicoll, V.J., 2007a, Distinct Taconic, Salinic, and Acadian deformation along the Iapetus suture zone, Newfoundland Appalachians: Canadian Journal of Earth Sciences, v. 44, p. 1567–1585.

Zagorevski, A., van Staal, C.R., McNicoll, V.J., and Rogers, N., 2007b, Upper Cambrian to Upper Ordovician peri-Gondwanan island arc activity in the Victoria Lake Supergroup, central Newfoundland: Tectonic development of the northern Ganderian margin: American Journal of Science, v. 307, p. 339–370.

Zagorevski, A., van Staal, C.R., Rogers, N., McNicoll, V.J., and Pollock, J., 2010, Middle Cambrian to Ordovician arc-backarc development on the leading edge of Ganderia, Newfoundland Appalachians: Geological Society of America Memoir, v. 206, p. 367–396.

Zaw, K., and Large, R.R., 1992, The precious metal-rich, South Hercules mineralization, western Tasmania: A possible subsea-floor replacement volcanic-hosted massive sulfide deposit: Economic Geology, v. 87, p. 931–952.